UNIVERSITAS INDONESIA

FORMATION AND CHARACTERIZATION OF ASYMMETRIC COMPOSITE CELLULOSE ACETATE /POLYSTYRENE MEMBRANE : Effect of surfactant as a template and its application for water desalination

DISSERTATION

Submitted as Partial Fulfillment of the Requirements for Doctoral Degree

Sri Mulijani
0606027985

FACULTY OF MATHEMATICS AND NATURAL SCIENCES
MATERIALS SCIENCE PROGRAM
JAKARTA
2010

STATEMENT OF THE ORIGINALITY

I hereby declare that this Dissertation is exclusively of my own original work, and all the sources those have been quoted or referred to have been correctly acknowledged

Name : Sri Mulijani
Student ID : 0606 027985

Signature :

Date :

University of Indonesia

APPROVAL PAGE

This dissertation is submitted by:

Name : **Sri Mulijani**

Student ID : **0606 027985**

Post Graduate Program : **Material Science Program**

Title :

FORMATION AND CHARACTERIZATION OF ASYMMETRIC COMPOSITE CELLULOSE ACETATE/ POLYSTYRENE MEMBRANE: Effect of Surfactant as a Template and its application for water desalination

has been successfully presented to the Examiner Committee as partial fulfillment of the requirements for Doctoral Degree at the Materials Science Program, Faculty of Mathematics and Natural Sciences, University of Indonesia.

EXAMINER COMMITTEE :

Promotor : Dr. Muhammad Hikam (.....)

Co Promotor : Dr.Emil Budianto (.....)

Examiner Committee:

Dr. Adi Basukriadi M.Sc. (Chair) (.....)

Dr. Soehardjo Poertadji (Member) (.....)

Dr. Bambang Soegijono (Member) (.....)

Dr. Kiagus Dahlan (Member) (.....)

Dr.Harini Sosiati (Member) (.....)

Approved in: Jakarta
Date: June 2, 2010

University of Indonesia

ACKNOWLEDGEMENT

First and foremost I would like to praise Allah SWT my lord for giving me the strength and patience to thoroughly finalize this dissertation with title:

FORMATION AND CHARACTERIZATION OF ASYMMETRIC COMPOSITE CELLULOSE ACETATE/POLYSTYRENE MEMBRANE: Effect of Surfactant as a Template and its application for water desalination

The writing of dissertation can be a lonely and isolating experience, yet it is obviously not possible without the personal and practical support of numerous people. I am especially indebted to my Promotor Dr. Muhammad Hikam and Co Promotor Dr. Emil Budianto for their continuous guidance, support, and inputs and throughout my doctorate program. I could not have written this dissertation without their strong encouragement and determination. They contributed their valuable time and efforts to review earlier drafts of my dissertation and answered numerous questions I had.

I would like to express my sincere gratitude to my dissertation examining committee members, Dr. Adi Basukriadi, M.Sc. Dean of Faculty of Mathematics and Natural Sciences University of Indonesia, Dr. Bambang Soegijono and Dr. Soehardjo Poertadji of Department of Physics FMIPA University of Indonesia, Dr. Harini Sosiati Technical Expert for Nanotechnology PT Sucofindo, and Dr. Kiagus Dahlan Vice of Dean Faculty of Mathematics and Natural Sciences Bogor Agricultural University Bogor. I am grateful for their willingness to contribute to my development, and to provide constructive feedback and thought provoking questions that helped to direct this research.

My special thanks extend to all lecturers and faculty in the Material Science Program for teaching me knowledge and skills to advance and complete my study.

I am truly indebted to the management of Chemistry Department Faculty of Mathematics and Natural Sciences Bogor agricultural University, for the support and the use of laboratory facilities to conduct this research work. My sincere gratitude goes to all staff in Inorganic Laboratory and Integrated

Laboratory. The completion of my research was also due to all your time and help.

Thanks also go to all my friends in the Material Science Program. I really enjoyed the friendships and fun we shared together. All those experiments and discussions we had had shown me what research really meant.

I would also like to extend my appreciation to all staff and the lab personnel at the Material Science Program of the Department of Physics FMIPA University of Indonesia for their helps and making my study so warm and memorable.

I want to thank my family for the love and support they have provided throughout my educational endeavors. A special thanks to my husband, my loving children, Sisy and Syifa, who have always been my biggest supporters; I know that without their love and encouragement, I could not have achieved this goal.

This dissertation may understandably be far from perfect, for which I encourage reviewers to provide feedbacks, suggestion or correction for any mistake, shortcomings or typos found in this work. I hope this research work will also be able to contribute and benefits to the advancement of sciences, in particularly in the field of material sciences.

Jakarta, June 2010
Sri Mulijani

STATEMENT PAGE
CONSENT TO PUBLISH FINAL RESEARCH WORK FOR ACADEMIC PURPOSE

Being part of the *civitas academica* of the University of Indonesia, the undersigned:

Name : Sri Mulijani

NPM : 0606027985

Program : Material Science

Department : Physics

Faculty : Mathematics and Natural Sciences

Paper : Dissertation

for the purpose of science development, agree to give to the University of Indonesia, a Non-exclusive Royalty Free Right on my scientific work entitled:

"FORMATION AND CHARACTERIZATION OF ASYMMETRIC COMPOSITE CELLULOSE ACETATE/POLYSTYRENE MEMBRANE: Effect of Surfactant as a Template and its application for water desalination"

including the software (when necessary). With this Non-exclusive Royalty Free Right University of Indonesia has the right to keep, to transform/format, to manage in the form of a database, to maintain and publish my final scientific work as long as it cite my name as the author/inventor and the owner of the Intellectual Property Right.

Prepared in: Jakarta

By

Sri Mulijani

University of Indonesia

ABSTRACT

Composite membrane nanofiltration for food industries, waste recovery and water desalination is a challenging application. The commercial membranes are relatively high cost. Therefore, there is a need to seek simple methods to provide low cost membranes. An alternative method to produce cellulose acetate (CA) membrane based on bacterial cellulose from pineapple waste was studied.

In this study, the effects of three surfactants, sodium dodecyl sulphate (SDS) as anionic surfactant, cetyl three methyl ammonium bromide (CTAB) as cationic surfactant and pluronic F127 as non-ionic surfactant on structure and performance of cellulose acetate-polystyrene membrane prepared from CA based on bacterial cellulose derived from nata de pine has been investigated. The process of preparation of membrane was done by immersion precipitation system. The morphology and performance of the prepared membranes were investigated using scanning electron microscopy (SEM), atomic force microscopy (AFM) and separation experiments using pure water and sea water as a feed. The results indicate that the small addition of surfactants in the casting solution increase the porosity of the membrane support layer, enhance pure water flux and sea water permeation. The SEM photographs showed that the surfactants played a crucial role in modifying the structure of membranes with different porosity and pore size. Membrane MCPT has bigger pore volume compared with that in others membranes. The study has proven that all of the membranes can be used for water desalination process. Rejection value test showed that membrane with addition of SDS has a higher rejection value than that of membrane MCPT and MCPl.

CONTENTS

LIST OF FIGURES

LIST OF TABLES

CHAPTER I
INTRODUCTION

1.1 Background

In 21st century, to solve these water problems, membranes technology is going to be further expanded. New technology further improvements of membrane performance, development of membrane systems, membranes stability such as antifouling membranes for wastewater treatment, and other highly qualified membranes will be needed. Membrane separation processes have become an essential part of the human life because of their growing industrial applications in high technology areas such as biotechnology, nano-technology and membrane-based energy devices. These processes are highly economically viable due to low energy requirements. Among these membrane processes, nanofiltration (NF) is the latest one developed. NF membranes possess a molecular weight cut-off of about a few hundreds to a few thousands Dalton which is intermediate between reverse osmosis and ultrafiltration membranes.

However, nanofiltration (NF) is one of parts of nanotechnology increasingly gaining attention in many separation and treatment processes such as water softening, color removal, chemical oxygen demand (COD) reduction and separation of medicines. NF membranes are often negatively charged, displaying separation characteristics in the intermediate range between reverse osmosis (RO) and ultrafiltration (UF). NF membranes generally have a thin skin layer enabling higher fluxes and lower operating pressures than RO membranes and are able to reject small organic molecules having molecular weights as low as 200–500 Da such as many medicines (streptomycin, penicillin etc.). Moreover, NF membranes are also able to reject ions, especially bivalent ions, due to the Donnan effect stemming from the membrane charge [1].

There are many methods for the preparation of composite membranes for NF including vapor deposition [2], plasma-initiated polymerization [3,4], photo-initiated polymerization [5], the radiation polymerization [6],the dip coating process [3], interfacial polymerization [7,8], electron beam irradiation [3], atom transfer radical polymerization [9], resin-filled chelating [10], and in situ amines cross-

linking [11]. Interfacial polymerization, however, is still a key method to produce commercial NF membranes such as the NF series (Filmtec Corporation), the NTR series (Nitto Denko Company), the UTC series (Toray Industries) and so forth. Although they have been used in many fields successfully, it should be an important promising work for membrane manufacturing to develop a novel NF membrane with special properties using high performance materials.

Special engineering plastics like poly(ether sulfone) (PES), polysulfone (PS), poly(vinylidene fluoride) (PVDF), and polyacrylonitrile (PAN) have become important NF membrane materials because of their good performances such as high mechanical property, good heat-aging resistance, and chemical stability[12]. However, NF membranes made of those materials have surfaces with not good wettability, resulting in the serious membrane fouling in many processes because of the solute–membrane hydrophobic interactions [13]. Accordingly, researchers have carried out hydrophilic modification of membrane surface with different methods like physical adsorption polymer blend, plasma modification, UV-assisted graft polymerization, X-ray-induced graft polymerization, and other chemical modification . Generally, surface hydrophilic modifications could obtain membranes with low fouling behavior and high flux. But some surface modifications might damage membrane structure and cause the decline of rejection and mechanical property.

Rapid development of nano-technology has dramatically increased great interest of some researchers to improve NF membrane performance through the incorporation of nanomaterials. Inorganic nanoparticles like TiO_2 [14–17] and Al_2O_3 [18] have been used to prepare nanocomposite membranes. These nanoparticles could improve the membrane hydrophilicity, thus the nanocomposite membranes were reported to have good antifouling performance. Electrospun PS, PVDF, PAN and poly(vinyl alcohol) nanofibers have also been used to prepare the filtration membranes [19–24]. Electrospun nanofibrous membranes possess some attractive attributes like high porosity, pore sizes ranging from tens of nanometer to several micrometers, interconnected open pore structure, and large surface area per unit volume [21]. Based on the above attributes, electrospun nanofibrous membranes get high flux. However, the electrospun nanofiber diameter is more than 100 nm

generally and the membranes are prepared by the simple collection of nanofibers, thus electrospun nanofibrous membranes have big pore size and could be only used to remove the micro-particle from solution by far. Compared with inorganic nanomaterials, organic nanomaterials have more functional groups. Thus, they could be easily bound with the hydrophobic polymers or be firmly fixed on substrate membranes through different chemical reactions. In addition, special functional groups of organic nanomaterials might give substrate membrane novel performance. Recently, nano-structure polyaniline (PANI) have attracted a great deal of interest because of their appealing potential applications in nano/microelectronics, sensors, and so on. In addition, as a desirable membrane material [25], PANI has been used to prepare gas separation [26], pervaporation [27,28], and semi-conductive membranes [29] because of its stability, relatively inexpensive cost, and simple acid–base doping chemistry [30,31]. PANI nanofibers could be prepared easily through polymerization reaction [32] and used to modify the material surface properties like hydrophilicity and charge on a nanoscale [33], which would be promising in the development of high flux and low fouling membranes.

As an agricultural country like Indonesia, membrane filtration for food industries, waste recovery and desalination is a challenging application. Although the cost of commercial membrane is now much lower than in the past ten years, it is still relatively high compared to agriculture products. This reason forms an obstacle to demonstrate membrane technology industrial uses. Even in education and research, membrane manufacturing is still costly due to imported substances, such as chemicals and polymers. Therefore, there is a need to seek simple methods and to provide cheap membranes. At least, their performance should sufficiently reliable for lab-scale usage for the first place. An alternative method to produce nanofiltration membranes based on cellulose bacteria was a trial in this study. Cellulose was converted to cellulose acetate through esterificatiion reaction.

It has been well known that bacteria, such as *Acetobacter*, *Rhizobium*, *Agrobacterium* and *Sarcina*, synthesize bio-polymers. Among those, gram negative *Acetobacter xyllinum* is claimed to be an effective cellulose-producing

bacterium and is widely used. It can be simply grown in a shallow tray with a culture medium; such as coconut juice, sugarcane juice, vinegar and fermented beverage, which are plentiful locally. The present research was based on utilization of pineapple garbage as a culture medium of *Acetobacter xyllinum* to produce cellulose bacteria. Cellulose network formed as a sheet floating on the medium surface that has been proved to have good properties: i.e. high tensile strength, high elasticity, high shape retention, high water binding capacity, non toxic and non allergen.

Cellulose acetate (CA), being an environment friendly product of sustainable resources, is an interesting polymer with respect to its low price, moderate chlorine resistance, good biocompatibility and high hydrophylicity. Due to its highly hydrophilic properties, it is known as a low fouling membrane for aqueous filtration [34]. Usually, CA membrane is prepared via the phase inversion technique. The first commercial membranes-based cellulose was made from cellulose acetate (CA) because there is no other low cost membrane. Basta Al. H (2008)[35] reported that, the problems associated with CA-membrane are its high rate of flux decline under operating conditions and time, as well as susceptibility to microbial degradation, causing rapid loss of semipermeability. Therefore, this type of membrane needs water pretreating by chlorine to prevent its biodegradation and held in a narrow pH-range (4–6) to avoid hydrolysis. The sensitivity and failure of CA membranes in presence of oxidizing agents, microorganisms, acid, operating high temperature, or alkaline pH-values is confirmed [36,37]. Also, biofouling on RO which is the most important application problem in the hot countries of the Middle East [38,39]. In view of their higher resistance to feed temperatures, high temperature reverse osmosis is shown to be a promising solution to biofouling of CA membranes parallel to the increase of permeation rate [40]. Unfortunately, it has been found that outside the pH-range (4–6), and as temperature is increased above 20^0C, the rate of hydrolysis of the acetate increased appreciably [41]. This leads to relative increases in the flux of salt and a consequent reduction in rejection [42]. In addition to the above problems, the stability of CA membranes in aqueous salt solution of various concentrations is of great importance to the process of reverse osmosis. Accordingly, a storage study

was indicated to ascertain whether or not the performance parameters and acetyl contents of a membrane changed over extended periods of storage in brine of varying concentration. The results of the study indicate that any hydraulic degradation, which occurs, is not effected by the saline solution [43].

In order to improve separation properties of CA membrane, many efforts have been made. Some researchers modified membranes through changing the solvent in the membrane casting solution [1,2,3,4,5,6]. Others tried to improve performance by employing different kind of additives or pore-forming agents. For instance, Arthanareeswaran et al. [44] prepared CA ultrafiltration membranes with polyethylene glycol 600 as an additive [45]. Sivakumar et al. succeeded in increasing water flux of CA-polysulfone blend ultrafiltration membranes by using polyvinylpyrrolidone as a pore-forming agent. Cailing Lv et al. studied to enhanced permeation performance of CA ultrafiltration membrane by incorporation of surfactant nonionic as a pore forming agent [34]

1.2 Objectives

The objectives of the present study are as follows:

1) to enhance performance of CA membrane resulted from esterification of bacterial cellulose obtained from nata the pine;
2) to determine the blending process of CA-PS;
3) to determine the residual surfactant content of the modified CA-PS membrane;
4) to determine the mechanical strength of the membrane;
5) to characterize the structural morphology of the membrane; and
6) to probe the rejection behaviour the membrane for its application of water desalination.

1.3 Scope of research

Research was performed to identify the performance of composite membrane. In this study used surfactant such as sodium dodecyl sulphate (SDS) as anionic surfactant, cetyle three methyl ammonium bromide (CTAB) as cationic surfactant and Pluronic F127 as non-ionic surfactant on structure and performance

of CA/PS membranes prepare from CA/PS/Acetone/dichloromethane system via immersion precipitation was investigated. The performance of membranes was studied by salt rejection behavior to obtain the value of Rejection Index (%Ri). Other observations were effect of surfactant toward morphology of membrane surface was conducted by AFM, SEM and FTIR measurement. Mechanical strength evaluated to observe strengthens of composite membranes.

1.4 Hypotheses

Phase inversion via immersion precipitation is well-known process for preparing a variety of asymmetric membranes. In this technique, a homogeneous polymer solution containing polymer and adequate solvent with or without an additive is casted on a glass plate and immersed in a coagulation bath (in some cases after a short period of solvent evaporation). The diffusive exchange solvent and non solvent introduces liquid-liquid phase separation, i.e. the formation of a polymer-rich and a polymer-lean phase in the casting solution lowers the Gibbs free energy of mixing. The successive solidification of the phase separated solution leads to a porous, asymmetric structure. The morphology and performance of membranes depend strongly on the thermodynamics as well as kinetics of phase inversion process.

The role of polymer precipitation is determined at each point by the progress of the concentration, which is in turn governed by interchange rate. Depending on the rate polymer precipitation, the following three types of membranes can be obtained:

(i) Symmetric, with an almost even porosity across the membrane cross-section.

(ii) Asymmetric, with a selective thin micro-porous upper layer on a thicker macro-porous globular or spongy sub-layer

(iii) Asymmetric, with large voids and /or finger-like cavities beneath the micro-porous upper layer.

A low precipitation rate leads to type (i) membranes, whereas a high precipitation rate results type (iii) membranes. One option for controlling the membrane formation process is introducing an additive in the casting solution. This study used surfactant as additive forming agent. Surfactants which are known

as surface-active agent matters reduce tension in water and other liquids (Yasemin, 2006). Surfactant-templated self-assembly of ordered nanoporous materials has been the focus of extensive research over the past decade. This simple and cost-effective approach has led to numerous morphological products with organized pore structures and a remarkable combination of high surface area (over 1000m2/g), uniform pore size distribution and precise tuning of pore size (2–30 nm). Control over the macroscopic morphology and the precise alignment of the inner nanochannels are significant factors to generate advanced products of commercial interest. The ultimate goal is to prepare this material as a supported thin film with nanochannels oriented vertical to the membrane surface.

CHAPTER 2
LITERATURE STUDY

2.1 Cellulose acetate

CA is one of important polymer used in industrial purposes. Commercially CA is made from processed wood pulp. The pulp is processed using acetic anhydride to form acetate flake from which products are made. Another technique for producing CA involved treating cotton with acetic acid, using sulfuric acid as a catalyst. Typical properties of CA polymer include: good toughness, deep gloss, high transparency and biodegradable. CA fibers are used for textiles and clothing. CA is organic ester cellulose (Figure 2.1a)

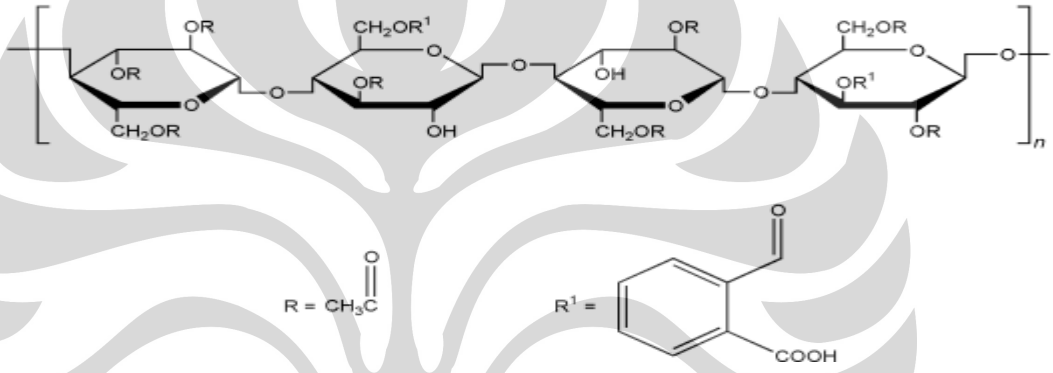

(a)

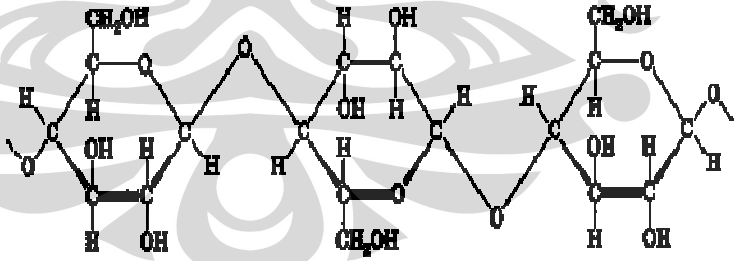

(b)

Figure 2.1a Sructure of CA; 1b. Sructure of Cellulose[89]

Cellulose has three hydroxyl group in the monomer of glucose anhydride (Figure 2.1b), that can be transformed to cellulose mono, di or tri acetate. Homogenous CA only obtained from substitution reaction –OH groups. The number of –OH groups substituted by acetyl groups has effluent to application of CA (Table 2.1)

Tabel 2.1a. Corelation of substitution degree, solvent and application of CA[89]

Substitution Degree	Solvent	Application of CA
0,6 - 0,9	Water	-
1,2 – 1,8	2-metoksietanol	plastic
1,8 – 1,9	Water-Propanol-Chloroform	Textile composite
2,2 – 2,3	Acetone	plastic
2,3 – 2,4	Acetone	fibers
2,5 – 2,6	Acetone	Film X-ray
2,8 – 2,9	Dichloromethane- ethanol	sheet
2,9 – 3	Dichloromethane	Textile

Tabel 2.1b Corelation of substitution degree and acetyl content

Substitution Degree	acetyl content (w%)
0.6-0.9	13.0-18.6
1.2-1.8	22.2-32.2
2.2-2.7	36.5-42.2
2.8-3.0	43.0-44.8

Source: Fengel *et al*. (1985)

2.2 Polystyrene[87]

Polystyrene was discovered in 1839 by Eduard Simon an apothecary in Berlin. From storax, the resin of the Turkish sweet gum tree (Liquidambar orientalis), he distilled an oily substance, a monomer which he named styrol. Several days later, Simon found that the styrol had thickened, presumably from oxidation; into a jelly he dubbed styrol oxide ("Styroloxyd"). By 1845 English chemist John Blyth and German chemist August Wilhelm von Hofmann showed that the same transformation of styrol took place in the absence of oxygen. They called their substance metastyrol. Analysis later showed that it was chemically identical to Styroloxyd. In 1866 Marcelin Berthelot correctly identified the

formation of metastyrol from styrol as a polymerization process. About 80 years went by before it was realized that heating of styrol starts a chain reaction which produces macromolecules, following the thesis of German organic chemist Hermann Staudinger (1881–1965). This eventually led to the substance receiving its present name, polystyrene.

The company I. G. Farben began manufacturing polystyrene in Ludwigshafen, Germany, about 1931, hoping it would be a suitable replacement for die-cast zinc in many applications. Success was achieved when they developed a reactor vessel that extruded polystyrene through a heated tube and cutter, producing polystyrene in pellet form.

2.2.1 Structure and properties

The chemical makeup of polystyrene is a long chain hydrocarbon with every other carbon connected to a phenyl group (the name given to the aromatic ring benzene, when bonded to complex carbon substituent's). Polystyrene's chemical formula is $(C_8H_8)n$; it contains the chemical elements carbon and hydrogen. Because it is an aromatic hydrocarbon, it burns with an orange-yellow flame, giving off soot, as opposed to non-aromatic hydrocarbon polymers such as polyethylene, which burn with a light yellow flame (often with a blue tinge) and no soot. Complete oxidation of polystyrene produces only carbon dioxide and water vapor.

This addition polymer of styrene results when vinyl benzene styrene monomers (which contain double bonds between carbon atoms) attach to form a polystyrene chain (with each carbon attached with a single bond to two other carbons and a phenyl group).

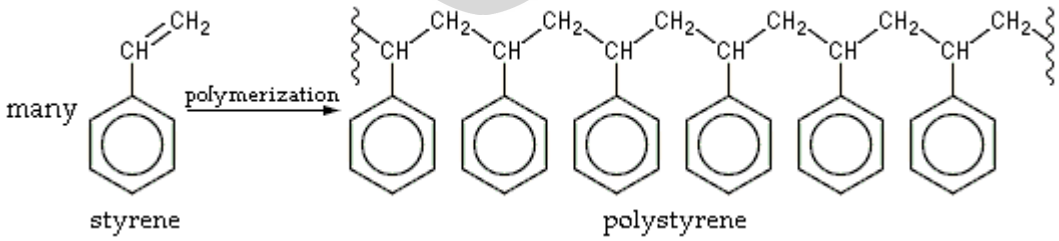

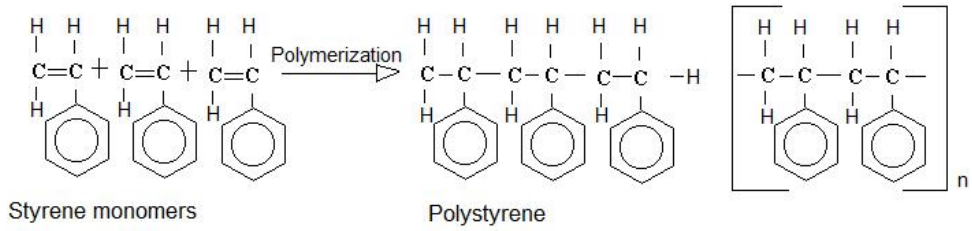

Figure 2.2 Structure of Polystyrene[87]

Polystyrene is chemically unreactive (this is why it is used to create products such as containers for chemicals, solvents and foods). This stability is the result of the transformation of carbon-carbon double bonds into less reactive single bonds. Structurally, the unsaturated alkene monomers have been transformed into less saturated structures with carbon alkane backbones. A molecule is considered saturated when its carbons are bonded to the maximum number of hydrogen atoms possible. The strong bonds within the molecule make styrene very stable.

Polystyrene is generally flexible and can come in the form of moldable solids or viscous liquids. The force of attraction in polystyrene is mainly due to short range van der Waals attractions between chains. Since the molecules and long hydrocarbon chains that consist of thousand of atoms, the total attractive force between the molecules is large. However, when the polymer is heated (or, equivalently, deformed at a rapid rate, due to a combination of viscoelastic and thermal insulative properties), the chains are able to take on a higher degree of conformation and slide past each other. This intramolecular weakness (versus the high intermolecular strength due to the hydrocarbon backbone) allows the polystyrene chains to slide along each other, rendering the bulk system flexible and stretchable. The ability of the system to be readily deformed above its glass transition temperature allows polystyrene (and thermoplastic polymers in general) to be readily softened and molded with the addition of heat.

A 3-D model would show that each of the chiral backbone carbons lies at the center of a tetrahedron, with its 4 bonds pointing toward the vertices. Say the -C-C- bonds are rotated so that the backbone chain lies entirely in the plane of the diagram. From this flat schematic, it is not evident which of the phenyl (benzene) groups are angled toward us from the plane of the diagram, and which ones are

angled away. The isomer where all of them are on the same side is called isotactic polystyrene, which is not produced commercially.

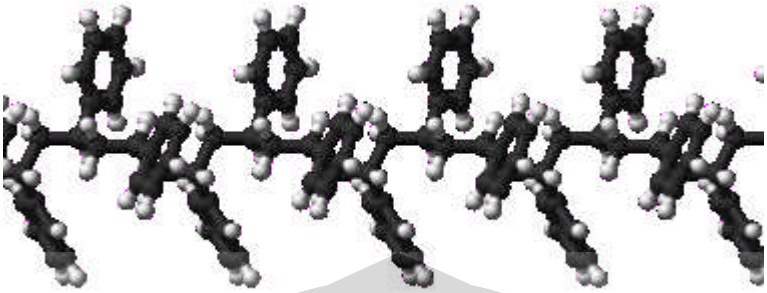

Figure 2.3 Structure 3D model of Polystyrene[87]

Ordinary atactic polystyrene has these large phenyl groups randomly distributed on both sides of the chain. This random positioning prevents the chains from ever aligning with sufficient regularity to achieve any crystallinity, so the plastic has a very low melting temperature, Tm<<TRT. But metallocene-catalyzed polymerization can produce an ordered syndiotactic polystyrene with the phenyl groups on alternating sides. This form is highly crystalline with a Tm of 270 °C (518 °F).

Table 2.2 Physical and chemical properties of Polystyrene[87]

Properties	
Density	1.05 g/cm3
Density of EPS	25-200 kg/m3
Dielectric constant	2.4–2.7
Electrical conductivity (s)	10−16 S/m
Thermal conductivity (k)	0.08 W/(m·K)
Young's modulus (E)	3000-3600 MPa
Tensile strength (st)	46–60 MPa
Elongation at break	3–4%
Glass temperature	95 °C
Melting point	240 °C
Specific heat (c)	1.3 kJ/(kg·K)
Decomposition	X years, still decaying

Polystyrene is commonly produced in three forms: extruded polystyrene, expanded polystyrene foam, and extruded polystyrene foam, each with a variety of applications. Polystyrene copolymers are also produced; these contain one or

more other monomers in addition to styrene. In recent years the expanded polystyrene composites with cellulose and starch have also been produced.

2.3 Membrane[46]

Membrane phenomena can be traced to the 18th century philosopher scientist. Abbé Nolet coined the word 'osmosis' to describe permeation of water through a diaphragm in 1748. Through the 19th and early 29th centuries, membranes had no industrial or commercial uses, but were used as laboratory tools to develop physical/chemical theories. Later, nitrocellulose membranes were preferred, because they could be made reproducibly. In 1907, Bechhold devised a technique to prepare nitrocellulose membranes of graded pore size, which it determined by a bubble test. Other early scientist, particularly Elford, Zsigmondy and Bachmann improved on Bechhold's technique, and by the early 1930s microporous membranes were commercially available [44]. During the next 20 years, this early microfiltration membrane technology was expanded to other polymers, notably cellulose acetate. Membrane found their first significant application in the testing of drinking water at the end of World War II. Drinking water supplies serving large communities in Germany and else where. By 1960, the elements of modern membrane science had been developed, but membranes were used in only a few laboratories and small, specialized industrial application. Membrane suffered from four problems that prohibited their widespread use as a separation process; they were too unreliable, too slow, too unselective, and too expensive. Solutions to each of these problems have been developed during the last 30 years, and membrane based separation processes are now commonplace[46].

The seminal discovery that transformed membrane separation from laboratory to an industrial process was the development, in early 1960. Loeb-Sourirajan (1960) (in Matsuura[45]) was developed preparing of membrane process which have defect free, high flux and anisotropic reverse osmosis membranes. This membrane consist of an ultrathin, selective surface film on a much thicker but much more permeable microporous support, which provides the mechanical strength.

Reverse osmosis membranes have been used widely for water treatment such as ultrapure water makeup, pure boiler water makeup in industrial fields, seawater and brackish water desalination in drinking water production, and wastewater treatment and reuse in industrial, agricultural, and indirect drinking water production as shown in Table 2.3.

Table 2.3 Application of Reverse Osmosis Membrane Process[45]

Industrial Use	Drinking Water	Wastewater Treatment and Reuse
Ultrapure water, boiler water, process pure water, daily industries	Seawater desalination, brackish water Desalination	Industrial water, agricultural water, indirect drinking water

The expansion of RO membrane applications promoted the redesign of suitable membrane material to take into consideration chemical structure, membranes configuration, chemical stability, and ease of fabrication. And along with the improvements of the membranes, the applications are further developed. Among desalination technologies available today, reverse osmosis (RO) is regarded as the most economical desalination process. Therefore, RO membranes have played crucial roles in obtaining fresh water from nonconventional water resources such as seawater and wastewater[45].

2.3.1 Membrane Classification[45,46]

Synthetic membranes for molecular liquid separation can be classified according to their selective barrier, structure, morphology and the membrane material. The selective barrier porous, nonporous, charged or with special chemical affinity dictates the mechanism of permeation and separation. In combination with the applied driving force for transport through the membrane, different types of membrane processes can be distinguished (Table 2.4).

Selective barrier structure. Transport through porous membranes is possible by viscous flow or diffusion, and the selectivity is based on size exclusion (sieving mechanism). This means that permeability and selectivity are mainly influenced by membrane pore size and the (effective) size of the components of the feed: Molecules with larger size than the largest membrane

pore will be completely rejected, and molecules with smaller size can pass through the barrier; the Ferry–Renkin model can be used to describe the effect of hindrance by the pore on rejection in ultrafiltration (UF) [44]. Transport through nonporous membranes is based on the solution-diffusion mechanism [44,46]. Therefore, the interactions between the permeand and the membrane material dominate the mass transport and selectivity. Solubility and chemical affinity on the one hand, and the influence of polymer structure on mobility on the other hand serve as selection criteria. However, the barrier structure may also change by uptake of substances from the feed (e.g., by plastification), and in those cases real selectivities can be much lower than ideal ones obtained from experiments using only one component in the feed or at low feed activities. Separation using charged membranes, either nonporous (swollen gel) or porous (fixed charged groups on the pore wall), is based on charge exclusion (Donnan effect; ions or molecules having the same charge as the fixed ions in the membrane will be rejected, whereas species with opposite charge will be taken up by and transported through the membrane). Therefore, the kind of charge and the charge density are the most important characteristics of these membranes [44]. Finally, molecules or moieties with special affinity for substances in the feed are the basis for carrier-mediated transport through the membrane; very high selectivity can be achieved; the diffusive fluxes are higher for (immobilized) liquid membranes than for polymer-based fixed-carrier membranes(44).

Concentration polarization can dominate the transmembrane flux in UF, and this can be described by boundary-layer models. Because the fluxes through nonporous barriers are lower than in UF, polarization effects are less important in reverse osmosis (RO), nanofiltration (NF), pervaporation (PV), electrodialysis (ED) or carrier-mediated separation. Interactions between substances in the feed and the membrane surface (adsorption, fouling) may also significantly influence the separation performance; fouling is especially strong with aqueous feeds.

Cross-section structure. An anisotropic membrane (also called .asymmetric.) has a thin porous or nonporous selective barrier, supported mechanically by a much thicker porous substructure. This type of morphology reduces the effective thickness of the selective barrier, and the permeate flux can

be enhanced without changes in selectivity. Isotropic (.symmetric.) membrane cross-sections can be found for self supported nonporous membranes (mainly ion-exchange) and macroporous microfiltration (MF) membranes (also often used in membrane contactors [44]. The only example for an established isotropic porous membrane for molecular separations is the case of track-etched polymer films with pore diameters down to about 10 nm. All the above-mentioned membranes can in principle be made from one material. In contrast to such an integrally anisotropic membrane (homogeneous with respect to composition), a thin-film composite (TFC) membrane consists of different materials for the thin selective barrier layer and the support structure. In composite membranes in general, a combination of two (or more) materials with different characteristics is used with the aim to achieve synergetic properties. Other examples besides thin-film are pore-filled or pore surface-coated composite membranes or mixed-matrix membranes.

Table 2.4 Overview of main polymer membrane characteristics and membrane-based processes for molecular separations in liquid phase(44,45,46).

		Transmembrane gradient		
Selective barrier	Typical structure	Concentration difference	Pressure difference	Electrical potential
Nonporous	anisotropic, thin-film composite	Pervaporation	Reverse osmosis Nanofiltration	
Microporous dp≤2nm	anisotropic, thin-film composite	Dialysis	Nanofiltration	Electrodialysis
Non- or microporous, with fixed charge	isotropic	Dialysis		Electrodialysis
Mesoporous dp= 2 . .50nm	anisotropic, isotropic track-etched	Dialysis	Ultrafiltration	Electroultrafiltration
Carrier in liquid	immobilized in isotropic porous membrane	Carrier-mediated separation		
Affinity ligand in solid matrix	isotropic, anisotropic			

Membrane materials. Polymeric membranes are still dominating a very broad range of industrial applications. This is due to their following advantages: (i) many different types of polymeric materials are commercially available, (ii) a large variety of different selective barriers, that is, porous, nonporous, charged and affinity, can be prepared by versatile and robust methods, (iii) production of large membrane area with consistent quality is possible on the technical scale at reasonable cost based on reliable manufacturing processes, and (iv) various membrane shapes (flat sheet, hollow-fiber, capillary, tubular, capsule; Figure 2.4) and formats including membrane modules with high packing density can be produced. However, membrane polymers also have some limitations. A very well-defined regular pore structure is difficult to achieve, and the mechanical strength, the thermal stability and the chemical resistance (e.g., at extreme pH values or in organic solvents) are rather low for many organic polymers. In that regard, inorganic materials can offer some advantages, such as high mechanical strength, excellent thermal and chemical stabilities, and in some cases a very uniform pore shape and size (e.g., in zeolites). However, some inorganic materials are very brittle, and due to complicated preparation methods and manufacturing technology, the prices for many inorganic membranes (especially those for molecular separations) are still very high. An overview of inorganic membranes for separation and reaction processes can be found elsewhere [47,48].

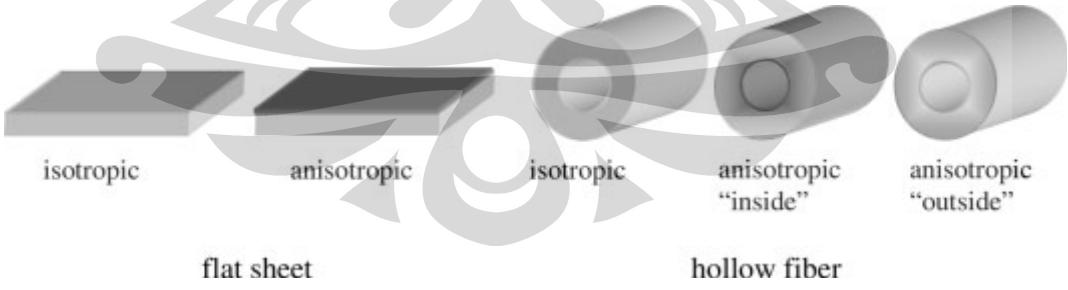

Figure 2.4 Polymeric membrane shapes and cross-sectional structures. Tubular membranes are similar to flat sheet membranes because they are cast on a macroporous tube as support. Capillary membranes are hollow fibers with larger diameter, that is, >0.5 mm[47,49].

2.3.2 Membrane Preparation[47,48]

2.3.2.1 Track-Etching of Polymer Films

Membranes with very regular pores of sizes down to around 10nm can be prepared by track-etching, in principle, those membranes can be used for the fractionation of macromolecules in solution. A relatively thin (<35 mm) polymer film (typically from poly(ethylene terephthalate) (PET) or aromatic polycarbonate (PC)) is first bombarded with fission particles from a high-energy source. These particles pass through the film, breaking polymer chains and creating damaged .tracks. Thereafter, the film is immersed in an etching bath (strong acid or alkaline), so that the film is preferentially etched along the tracks, thereby forming pores. The pore density is determined by irradiation intensity and exposure time, whereas etching time determines the pore size. The advantage of this technique is that uniform and cylindrical pores with very narrow pore-size distribution can be achieved. In order to avoid the formation of double or multiple pores, produced when two nuclear tracks are too close together, the membrane porosity is usually kept relatively low, that is, typically less than 10%.

2.3.2.2 Phase Separation of Polymer Solutions

Polymer membranes by phase separation. The method is often called .phase inversion, but it should be described as a phase-separation process: a one-phase solution containing the membrane polymer is transformed by a precipitation/solidification process into two separate phases (a polymer-rich solid and a polymer-lean liquid phase). Before the solidification, usually a transition of the homogeneous liquid into two liquids (liquid–liquid demixing) occurs. The “proto-membrane” is formed from the solution of the membrane polymer by casting a film on a suited substrate or by spinning through a spinneret together with a bore fluid. Based on the way the polymer solution is solidified, the following techniques can be distinguished[47,48]:

(i) Nonsolvent-induced phase separation (NIPS) the polymer solution is immersed in a nonsolvent coagulation bath (typically water); demixing and precipitation occur due to the exchange of solvent (from polymer

solution) and nonsolvent (from coagulation bath), that is, the solvent and nonsolvent must be miscible.

(ii) Vapor-induced phase separation (VIPS) the polymer solution is exposed to an atmosphere containing a nonsolvent (typically water); absorption of nonsolvent causes demixing/precipitation.

(iii) Evaporation-induced phase separation (EIPS) the polymer solution is made in a solvent or in a mixture of a volatile solvent and a less volatile nonsolvent, and solvent is allowed to evaporate, leading to precipitation or demixing/ precipitation.

(iv) Thermally induced phase separation (TIPS) a system of polymer and solvent is used that has an upper critical solution temperature; the solution is cast or spun at high temperature, and cooling leads to demixing/precipitation.

By far the majority of polymeric membranes, including UF membranes and porous supports for RO, NF or PV composite membranes, are produced via phase separation. The TIPS process is typically used to prepare membranes with a macroporous barrier, that is, for MF, or as support for liquid membranes and as gas–liquid contactors. In technical manufacturing, the NIPS process is most frequently applied, and membranes with anisotropic cross-section are obtained. Often, the time before contact with the coagulation bath is used to "fine tune" membrane pore structure; some of these processes can thus be described as combinations of VIPS followed by NIPS.

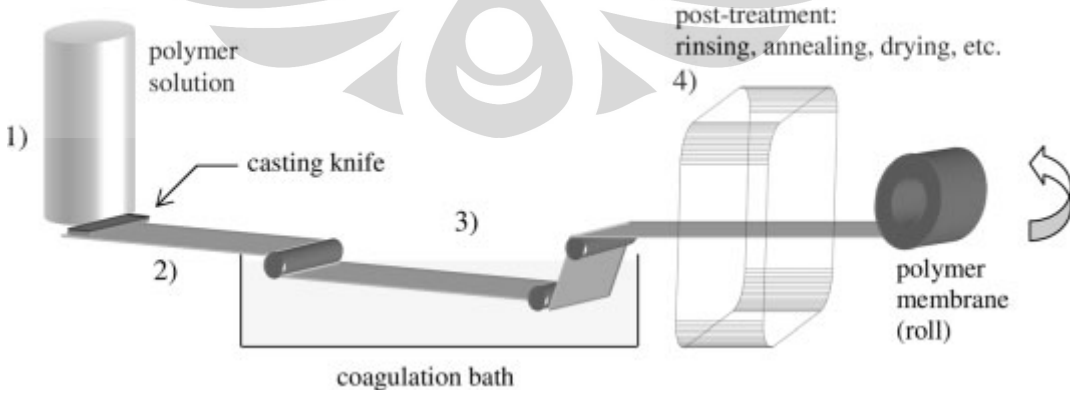

Figure 2.5 Schematic depiction of the continuous manufacturing process of polymeric membranes by the NIPS process[47,48].

Integrally anisotropic polymer membranes via NIPS process. The cross-sectional structure of an anisotropic membrane is crucial in order to combine the desired selectivity (by a barrier with pores in the lower nm range or by a nonporous polymer) with high fluxes: the top layer acts as a thin selective barrier and a porous sublayer provides high mechanical strength. Such integrally "asymmetric" membranes were first discovered by Loeb and Sourirajan [58]. This finding was the first breakthrough for commercial membrane technology, that is, such RO membranes from CA showed much higher fluxes than the previously produced ones from the same polymer. This method involves (Figure 2.5): (1) polymer dissolution in single or mixed solvent, (2) casting the polymer solution as a film (.proto-membrane.) on suited substrate (or spinning as free liquid film, for hollow fiber), (3) precipitation by immersion in a nonsolvent coagulation bath, and (4) post-treatments such as rinsing, annealing and drying. The membranes resulting from this process have typically a very thin (<1 mm, often even less than 100 nm) top skin layer (selective barrier), which is either nonporous or porous (Figure 2.6).

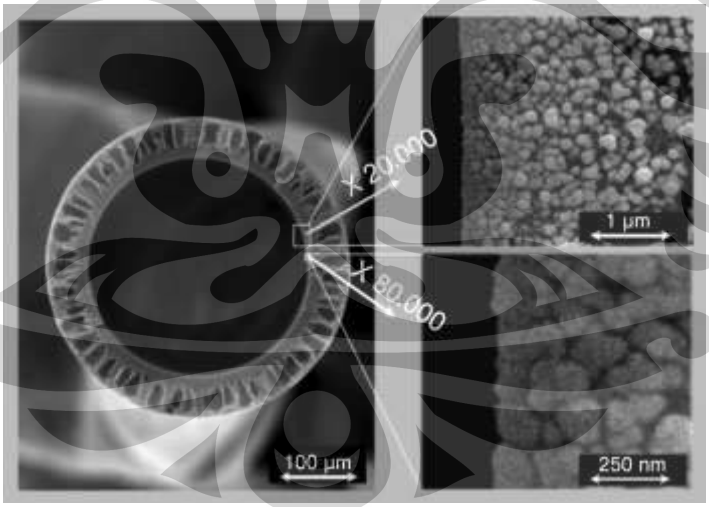

Figure 2.6 SEM micrograph of a cross-section of a hollow-fiber dialysis membrane (Polyflux, Gambro) with an anisotropic structure and macrovoids in the support layer (left), and details of the inner porous separation layer in two different magnifications(47)

The selection of the materials and the discussion of mechanisms for phase separation are based on ternary phase diagrams with the three main components polymer, solvent and nonsolvent; a pronounced miscibility gap (instable region) is

an essential precondition. Besides thermodynamics aspects, the onset and rate of precipitation in the liquid film (both are different depending on the distance to the plane of first contact with the coagulation bath) are also important; the mass transfer (nonsolvent in-flow, and solvent out-flow) can have tremendous influence. Two mechanisms are distinguished: (i) instantaneous liquid–liquid demixing, which will result in a porous membrane, (ii) delayed onset of liquid–liquid demixing, which can result in a membrane with a nonporous barrier skin layer [46]. The rate of precipitation decreases from the top surface (in most cases, this plane of first contact with the coagulation bath will be the barrier in the final membrane) to the bottom surface of the cast film. As precipitation slows down, the resulting pore sizes increase because the two phases have more time to separate. In practice, most systems for membrane preparation contain more than three components (e.g., polymer blends as materials and solvent mixtures for casting solution and coagulation bath)[47,48].

Characteristics of the casting solution. Most important is the selection of a suitable solvent for the polymer, that is, the strength of mutual interactions is inversely proportional to the ease of precipitation by the nonsolvent. Polymer concentration also plays a vital role to determine the membrane porosity. Increasing polymer concentration in the casting solution leads to a higher fraction of polymer and consequently decreases the average membrane porosity and pore size. In addition, increasing the polymer concentration could also suppress macrovoid formation and enhance the tendency to form sponge-like structure. However, this can also increase the thickness of the skin layer. Even though details depend on the properties of the membrane polymer,UFmembranes can be obtained within a range of polymer concentrations of 12–20 wt%, whereas RO membranes are typically prepared from casting solutions with polymer concentrations ≥20 wt% (in order to increase salt rejection, a thermal annealing step is often added to the manufacturing scheme).

Solvent/nonsolvent system. The solvent must be miscible with the nonsolvent (here an aqueous system). An aprotic polar solvent like N-methyl pyrrolidone (NMP), dimethyl formamide (DMF), dimethyl acetamide (DMAc) or dimethylsulfoxide (DMSO) is preferable for rapid precipitation (instantaneous

demixing) upon immersion in the nonsolvent water. As a consequence, a high porosity anisotropic membrane can be achieved. For slow precipitation, yielding low porosity or nonporous membrane, solvents having a relatively low Hildebrand solubility parameter like tetrahydrofuran (THF) or acetone are preferable.

Additives. For certain purposes, additive or modifier is added in the casting solution. Indeed, this additive can determine the performance of the ultimate membrane and is often not disclosed for commercial membranes. Usually, additives include (i) co solvent with relatively high solubility parameter (such a solvent can slow down the precipitation rate, and higher rejection is achieved), (ii) pore-forming agents such as poly(vinyl pyrolidone) (PVP) or poly(ethylene glycol) (PEG) (these hydrophilic additives can enhance not only membrane pore size but also membrane hydrophilicity; at least partially, these polymers form stable blends with membrane polymers such as PSf or PES), (iii) nonsolvent (should be added only in such amounts that demixing of the casting solution does not occur; promotes formation of a more porous structure and could also reduce macrovoid formation), (iv) addition of crosslinking agent into casting solution (is less frequently used, but could also reduce macrovoid formation).

Characteristics of coagulation bath. The presence of a fraction of solvent in the coagulation bath can slow down the liquid–liquid demixing rate. Consequently, a less porous barrier structure should be obtained. However, the opposite effect can also occur, that is, addition of solvent can decrease polymer concentration (in the proto membrane) leading to a more open porous structure. The amount of the solvent to be added strongly depends on the solvent_nonsolvent interactions. As the mutual affinity of solvent and nonsolvent increases, more solvent is required to achieve an effect on the membrane structure. For example, in preparation of CA membranes, the content of solvent needed in a coagulation bath for a DMSO/water system is higher than for a dioxan/water system. Instantaneous demixing resulting in a porous structure can be obtained by better miscibility between solvent and nonsolvent. In contrast, a less miscible solvent/nonsolvent combination results in a more nonporous structure. Furthermore, addition of solvent into a coagulation bath could also

reduce the formation of macrovoids leading to the desired, more stable sponge-like structure of the supporting layer.

Exposure time of proto-membrane before precipitation. The effect of exposure to atmosphere before immersion is dependent on the solvent property (e.g., volatility, water absorption) and atmosphere property (e.g., temperature, humidity). This step (i.e., combination of EIPS or VIPS with NIPS; cf. above) has significant effects on the characteristics of the skin layer and the degree of anisotropy of the resulting membrane.

2.4 Composite Membrane Preparation[59]

Composite membranes combine two or more different materials with different characteristics to obtain optimal membrane performance. Basically, the preparation involves: (i) preparation of porous support that is usually made by a phase-separation process , and (ii) deposition of a selective barrier layer on this porous support. A number of methods are currently used for manufacturing asymmetric composite membranes, which will be briefly explained as below [59.] .

(i) Laminating. An ultrathin film is cast and then laminated to a (micro) porous support. This method has been used for preparing early RO membranes for water desalination.

(ii) Dip-coating of a polymer solution onto a support microporous support is followed by drying, or a reactive prepolymer is applied and IR radiation is used for curing. As a result, a thin layer of the coated polymer on the substrate is obtained. In some cases, crosslinking is done during curing to increase mechanical or chemical stability. Two problems are often observed, that is, penetration of the dilute coating solution into the pores of the support and formation of defective coatings. The first problem can be reduce by precoating the support with a protective layer from a hydrophilic polymer, such as polyacrylic acid or by filling the pores with a wetting liquid such as water or glycerin. The latter problem can be reduced by introducing an intermediate layer between the selective polymer film and the porous substrate.

(iii) Plasma polymerization. Gas-phase deposition of the barrier layer on a porous support is conducted from glow-discharge plasma via plasma polymerization. This method has been successfully used for RO membrane preparation [19].

(iv) Interfacial polymerization. This method has been developed by Cadotte et al. [59], and it is now the most important route to RO and NFmembranes. The selective layer is formed in situ by polycondensation or polyaddition of reactive (bis- and trisfunctional) monomers or prepolymers on the surface of a porous support (Figure 2.7). Post-treatment such as heating is often applied in order to obtain a fully cross-linked structure of the selective barrier.

Other methods derived from surface modification, including heterogeneous graft copolymerization or in situ radical polymerization and deposition of polyelectrolyte.

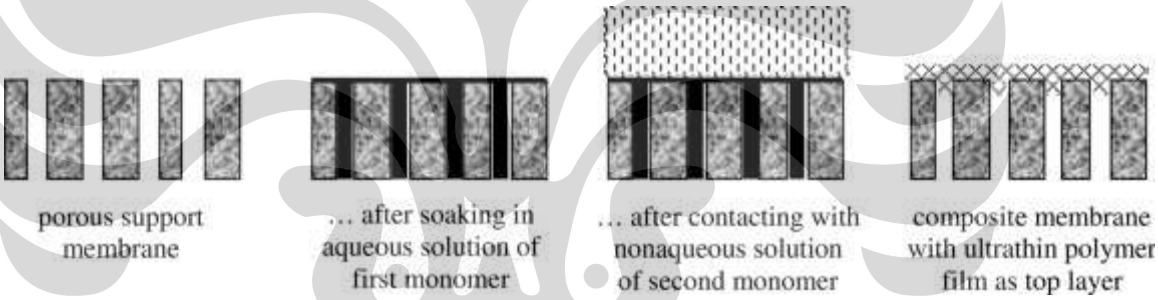

Figure 2.7 Schematic depiction of the preparation of TFC membranes by interfacial polymerization: The support membrane (e.g., bis- or trifunctional amine), and subsequently contacted with a second bath containing a water-immiscible solvent in which another reactive monomer or prepolymer has been dissolved (e.g., bis- or trifunctional carbonic acid chloride). The reaction takes place at the interface of the two immiscible solutions on the outer surface of the support membrane, and the thickness of the polymer layer (e.g., cross-linked polyamide) is limited by its barrier properties for further diffusion of reactants into the reaction zone[(59)].

2.5 Membrane Modification[(59)]

Because most of the established membrane polymers can not meet all the performance requirements for a membrane dedicated to a particular application, membrane modifications are gaining rapidly increasing importance. Membrane modification is aimed either to minimize undesired interactions, which reduce membrane performance (e.g., membrane fouling), or to introduce additional

interactions (e.g., affinity, responsive or catalytic properties) for improving the selectivity or creating an entirely novel separation function. Three general approaches can be distinguished:

(i) Chemical modification of the membrane polymer (for membrane formation),

(ii) Blending of the membrane polymer with other polymer(s) (before membrane formation), and

(iii) Surface modification after membrane preparation.

An important example of polymer modification before membrane formation is sulfonation or carboxylation, for example, of PSf or PES, to obtain a more hydrophilic ultrafiltration membrane from a very stable membrane polymer [23]. The most well-known example for blending with the membrane polymer is the use of the water-soluble PVP during manufacturing of flatsheet or hollow-fiber membranes from PSf or PES [24]. Even though during the coagulation and washing steps, some of the added modified or other polymer can leach out from the membrane matrix, a fraction remains on the pore surface and thus enhances the membrane hydrophilicity. Recently, amphiphilic graft or block copolymers containing functional (surface active) macromolecule segments and other segments that are compatible with the bulk of the membrane polymer have been introduced as .tailored. macromolecular additives to render the final membrane surface hydrophilic or hydrophobic [60, 61].

2.5.1 Cellulose Acetate Membrane[44,45,47]

Reverse osmosis systems were originally presented by Reid in 1953. The first membrane, which could be used at the industrial level in actual water production plants, was a cellulose-acetate-based RO membrane invented by Loeb and Sourirajan in 1960. This membrane has a so-called asymmetric or anisotropic membrane structure having a very thin solute-rejecting active layer on a coarse supporting layer, as shown in Figure 2.8.

The membrane is made from only one polymeric material, such as cellulose acetate, and made by the nonsolvent-induced phase separation method.

After the invention by Loeb and Sourirajan, spiral-wound membranes elements using the cellulose acetate asymmetric flat-sheet membranes were developed and manufactured by several U.S. and Japanese companies. RO technologies have been on the market since around 1964 [58]. They were widely used from the 1960s through the 1980s mainly for pure water makeup for industrial processes and ultrapure water production in semiconductor industries; and some are still used in some of these applications.

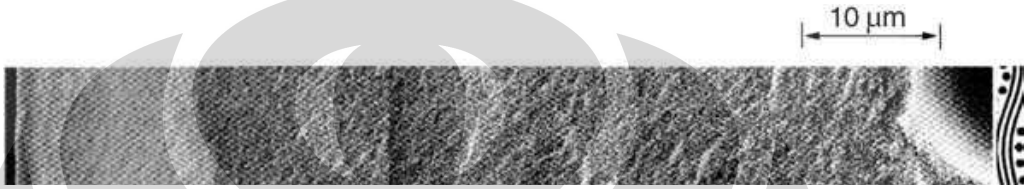

Figure 2.8 SEM photograph of CA asymmetric membrane(47,48)

2.5.2 Composite Membrane(47,48)

Another approach to obtain a high-performance RO membrane was investigated by some research institutes and companies in the 1970s. Many methods to prepare composite membranes have been proposed, as shown in Table 1.2. In the early stage, very thin films of a cellulose acetate (CA) polymer coating on a substrate, such as a porous cellulose nitrate substrate, was tried. However, in spite of their efforts, this approach did not succeed in industrial membranes manufacturing.

Another preparation method for composite membrane is an in situ monomer condensation method using the monomeric amine and monomeric acid halide, which was also invented by Cadotte. Then, many companies succeeded in developing composite membranes using this method, and the membrane performance has been drastically improved up to now. Now, composite membrane of cross-linked fully aromatic polyamide is regarded as the most popular and reliable material in the world. Permeate flow rate and its quality have been improved 10 times greater than that of the beginning [58].

Figure 2.9 shows recent trends in RO membrane technology with two obvious tendencies. One is a tendency toward low-pressure membranes for operating energy reduction in the field of brackish water desalination. The other is

a tendency toward high rejection with high-pressure resistance in the large seawater desalination market.

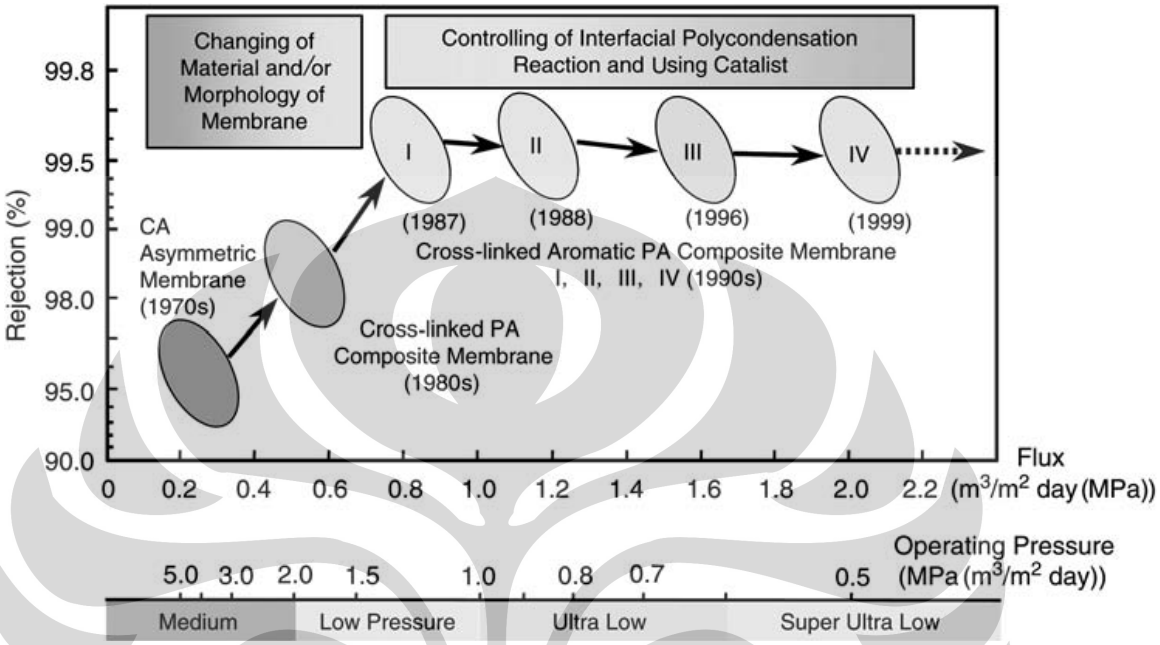

Figure 2.9 Performance trends in RO membrane for brackish water desalination[58].

Figure 2.9 shows the progress of low-pressure membrane performance trends in RO membrane on brackish water desalination from the 1970s to the 1990s, including industrial water treatment such as ultrapure water production. In the 1970s much effort was devoted to developing high-performance membrane materials and improving the membrane performance.

The progress of RO membranes for seawater desalination is shown in Figure 2.10[58]. It is very important to increase the water recovery ratio on seawater desalination systems to achieve further cost reduction. Most seawater RO desalination systems in use today are confined to approximately 40% conversion of the feed water (salt concentration 3.5%), since most of commercially available RO membrane do not allow for high-pressure operation of more than around 7.0MPa. Recent progress on high-pressure–high-rejection spiral wound (SW) RO elements, combined with proven and innovative energy recovery

and pumping devices, has opened new possibilities to reduce investment and operating cost.

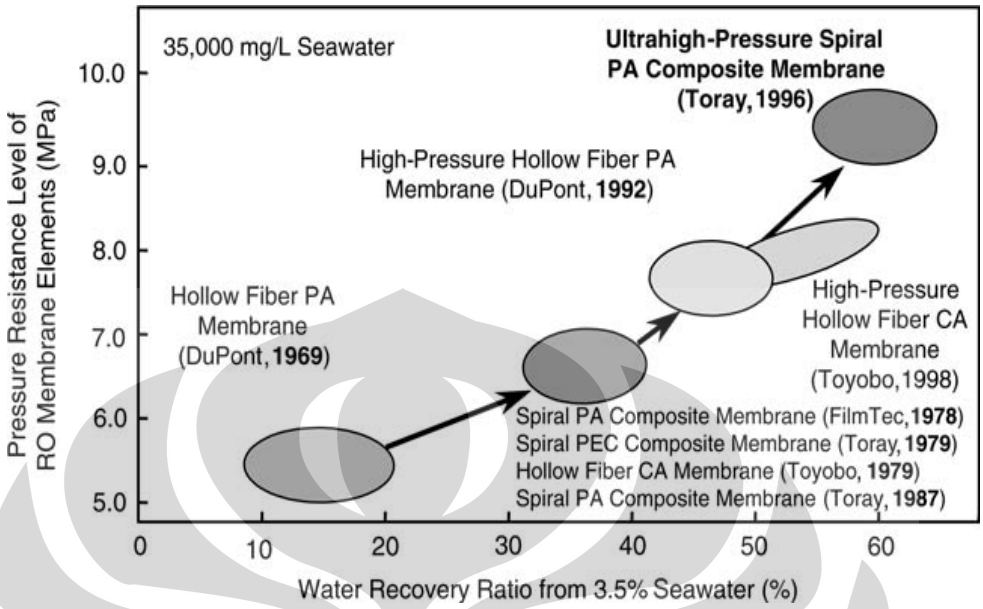

Figure 2.10 Performance trends in RO membranes for seawater desalination[58]

2.6 Nanofiltration[62,63]

The history of nanofiltration (NF) dates back to the 1970s when efforts started to develop reverse osmosis (RO) membranes with a reasonable water flux at relatively low pressures. The high pressures used in reverse osmosis resulted in a considerable energy cost, but, on the other hand, the quality of the obtained permeate was very good, and often even too good. Thus, membranes with lower rejections of dissolved components, but with a higher water permeability, would be a great improvement for separation technology. Such low-pressure RO membranes became known as nanofiltration membranes. By the second half of the 1980s, nanofiltration slowly started to come of age.

In comparison with ultrafiltration (UF) and reverse osmosis, nanofiltration has always been a difficult process to define and to describe. Tight NF membranes are in some ways similar to RO membranes, and loose NF membranes could probably be classified as UF membranes. The specific features of NF membranes are mainly the combination of very high rejections for multivalent ions (.99%) with low to moderate rejections for monovalent ions (0–70%), and the high rejection (.90%) for organic compounds with a molecular weight above the

molecular weight of the membrane, which is usually in the range of 150–300. However, nanofiltration is still a gray zone in terms of physicochemical interactions and transport mechanisms; a transition zone with features of both UF and RO, but with its own particular characteristics as well. Understanding these phenomena is a challenge for researchers and product developers.

In the second half of the 1990s, research on nanofiltration increased. As a consequence, scientists and industrialists nowadays feel more confident about what can be expected from a nanofiltration membrane, and more and more applications proved to be successful. By 2000, the installed capacity was about 6000 ML/day, which is 10 times higher than in 1990 [62]. As research continues, membranes become better defined, less prone to fouling, and more resistant to harsh conditions. Examples are the development of ceramic NF membranes and polymeric solvent-resistant nanofiltration (SRNF) membranes. Taking the number of possible applications in, for example, the chemical and pharmaceutical industry into account, in addition to the applications that are still to be implemented but can be considered as state-of-the-art, it can be assumed that the increase of installed capacity will continue for many more years.

The traditional materials used for NF membranes are organic polymers. NF membranes are made by phase inversion or by interfacial polymerization [63]. Phase inversion membranes are homogeneous and asymmetric and often made of cellulose acetate or poly(ether)sulfone. Membranes made by interfacial polymerization are heterogeneous: They consist of a thin-film composite layer on top of a substrate UF layer. Typical polymers are (aromatic) polyamides, polysulfone/poly(ether sulfone)/sulfonated polysulfone, polyimide, and poly(piperazine amide); other polymers or blends can be used as well. Recent trends are the use of highly cross-linked polymers in order to obtain enhanced membrane stability at low or high pH, at high temperature or in organic solvents. NF membranes contain functional groups that can be charged, depending on the pH of the solution in contact with the membrane. Typically, NF membranes are negatively charged at neutral pH, with the isoelectric point around pH 3–4.

The production of ceramic NF membranes is also possible, but to date the pore size of most ceramic NF membranes is still relatively high. The molecular

weight cutoff, the molecular weight of a component retained by 90%, is usually above 500 [64,65,66]. Molecular weight cutoff (MWC) values of 200 and below were recently reported for Al_2O_3/TiO_2 membranes [67]. These membranes were obtained by a careful preparation of each sublayer. The macroporous substrate consisted of a-Al_2O_3; the intermediate layers were prepared from TiO_2, a-Al_2O_3, g-Al_2O_3, or mixtures or these components; the top layer is a fine textured polymeric TiO2 top layer. Most NF membranes are packed into spiral-wound elements; however, tubular, hollowfiber, and flat-sheet or plate-and-frame modules are also available [58]. Tubular membranes with diameter around 1 mm, denoted as capillary membranes, are interesting in view of fouling control.

2.6.1 Performance[62,63]

Three parameters are crucial for the operation of a (nano) filtration unit: solvent permeability or flux through the membrane, rejection of solutes, and yield or recovery. The flux J or the permeability (flux per unit of applied pressure) of a membrane is, similarly to other pressure-driven membrane processes, a crucial parameter. Most NF membranes except some used for solvent applications are hydrophilic. If the Hagen–Poiseuille equation can be assumed (although this equation is, in fact, only valid for porous membranes), the other parameters influencing the permeability are obvious:

$$J = \frac{\varepsilon\, r^2 \Delta P}{8\, \eta\, \tau\, \Delta x} \qquad (1)$$

A large membrane surface porosity (ε), large pore radii (r), and a low tortuosity (t), together with a low membrane thickness Δx, are advantageous. The influence of the viscosity (η) is important when the temperature is varied: a lower viscosity is obtained at higher temperatures, which results in higher fluxes. An increase of the temperature by 18°C corresponds to a flux increase of 2–2.5%. For concentrated solutions or solutions with high salinity, the osmotic pressure ΔP should be subtracted from the applied pressure ΔP. The flux equation then becomes

$$J = Lp\,(\Delta P - \sigma\, \Delta\pi) \qquad (2)$$

where Lp is the solvent permeability and s is the (maximal) rejection of the solute. The osmotic pressure can be calculated by using the Van't Hoff equation [46] or, with more precision, by using the Pitzer model [46]. A similar transport equation can be written for the solute:

$$Js = Ps\,\Delta x\,\frac{dc}{dx} + (1-\sigma)Jc \qquad (3)$$

where c is the concentration of the solute and *Ps* is the permeability of the solute. Transport by diffusion is represented by the first term in this equation; the second term stands for the contribution of convection to the transport of (uncharged) molecules.

The rejection of component *i* is defined as

$$Ri(\%) = (1 - \frac{Cp,i}{Cf,i}) \text{ x } 100 \qquad (4)$$

where *Cp,i* is the permeate concentration and *Cf,i* is the feed concentration of component i; *R* is a dimensionless parameter and its value normally varies between 100% (complete rejection of the solute) and 0% (solute and solvent pass freely through the membrane).Negative rejections can sometimes be observed when the solute passes favorably through the membrane, for example, in salt mixtures.

The rejection of a given molecule can be calculated from the equations above as

$$R = \frac{\alpha \ldots (1-f)}{1-\alpha f} \qquad (5)$$

$$F = \exp\,(-\frac{1-\alpha}{Ps}\,J) \qquad (6)$$

The rejection in NF is mainly determined by molecular size, hydrophobicity, and charge [68,69,70,71] , but effects of, for example, molecular shape and dipole moment, might play a role as well. The pore/void dimensions are statistically distributed and can be described by a log-normal distribution [70]. This explains the

smooth transition from no rejection to complete rejection in a typical S-shaped curve when molecular size is varied. The MWC value is often used to indicate the lower limit of molecules that are (almost completely) retained, similar to UF membranes. For NF membranes, with MWC values between 150 and 1000 (but often in the range 150–300), this concept should be used with care: Hydrophobic molecules larger than the MWC, for example, often have a low rejection; the pH of the solution might change the membrane's surface charge as well as the charge of the solute, so that the rejection of this solute can be higher or lower than expected. The third important parameter is the recovery or yield. This is a parameter for the design of an industrial application rather than a membrane characteristic. The recovery is the ratio of the permeate stream to the feed stream; its value ranges from 40 to 90%.

2.7. Fouling in Membrane Processes[74,75]

The processes of membrane fouling with particular reference to the pressure driven liquid-phase membrane processes where the solvent is water are low-pressure microfiltration (MF) and ultrafiltration (UF) and highpressure nanofiltration (NF) and reverse osmosis (RO). Fouling presents as a decrease in membrane performance with a loss in solvent permeability and changes to solute transmission. Fouling is caused by deposition of feed components, or growth (as in biofouling and scale formation) onto or into the membrane; it is a widespread and costly problem. The foulant membrane interaction depends on the nature of the foulant, the membrane and the operating environment. This section provides an overview of fouling and describes various generic fouling mechanisms.

2.7.1. Membrane Fouling in NF[74,75]

A problem often encountered in practical applications of NF is the decrease of the water flux for real feed solutions in comparison to the pure water flux. Flux decline can be caused by membrane fouling [72]. Fouling is caused by precipitation of inorganic components such as $CaCO_3$ or $CaSO_4$ [73,74], deposition of organic compounds [74], or possibly growth of bacteria on the membrane surface (biofouling) [75]. Fouling can be defined as irreversible flux decline that

can only be removed, for example, by chemical cleaning. When flux decline disappears by simply changing the feed solution to pure water, the phenomenon is reversible and should therefore not be considered as fouling. Both reversible flux decline and fouling cause practical problems in the application of nanofiltration: For a given membrane surface, the yield of permeate decreases; the energy consumption increases because higher pressures are needed to obtain the same flow rate; cleaning procedures need additional chemical reagents; and the lifetime of the membrane decreases. Furthermore, the rejection of different components might change. It might be expected that rejections generally increase when flux decline occurs, for example, because of pore narrowing, but this is not always the case.

Flux decline due to the presence of organic compounds in the feed solution was, for example, encountered in nanofiltration of surface water containing high concentrations of natural organic matter (NOM) [76,77], where interactions between organic compounds and the membrane material (in a hollowfiber module) even lead to the formation of a cake layer. This was also reported for groundwaters and for surface waters during nanofiltration with spiral-wound membranes [78]. It is usually accepted that flux decline in aqueous solutions containing organic molecules is mainly caused by adsorption, possibly enhanced by pore blocking [79,71]. Adsorption on NF membranes has been related to high-performance liquid chromatography (HPLC) characteristics [80]. Similar problems have been reported for UF membranes and for RO membranes [58]. For ultrafiltration, it was found that molecular size is the most important factor determining flux decline, whereas in reverse osmosis different factors reflecting hydrophobicity play a role.

One of the main problems still to be solved for nanofiltration, and for pressure-driven membrane filtration in general, is the further treatment of the concentrate fraction [79]. The relative volume of the concentrate may range from 40 to 90% of the feed volume; its composition is similar to the feed, but the concentration factor (CF) of rejected compounds is higher by a factor CF calculated as

$$CF = \frac{Cr,i}{Cf,i} = \frac{Qf}{Qr}[1 - REC(\frac{Cp,i}{Cf,i}) \qquad (7)$$

where Q is the volumetric flow (L/h) and C is the concentration (mg/L); the subscripts r, f, p, and i refer to the concentrate (or retentate), the feed, the permeate, and the component used, respectively, and REC is the relative fraction of the permeate compared to the feed. For components that are completely rejected, this equation simplifies to

$$CF = \frac{1}{1 - REC} \qquad (8)$$

As a consequence of this large variation, the further environmental fate of the concentrate is unpredictable; a large variation in possibilities for reuse, further treatment, or discharge exists. Cost factors and legal aspects also play an important role. Generally, all methods for concentrate processing can be classified into one of the following categories [79]: (1) reuse, (2) further treatment by removal of contaminants, (3) incineration, (4) direct or indirect discharge in surface water, (5) direct or indirect discharge in groundwater, and (6) landfilling. Reuse is the most attractive option but only applicable in a few cases where the concentrated fraction is actually the desired product, such as in the food industry (e.g., dairy products, starch processing). The permeate is then a side product, which can be reused as a rinsing water or discharged. If reuse of the concentrate is not possible, further treatment may be necessary before discharge. Two options for further treatment can be distinguished: (a) water removal from the concentrate and (b) removal of specific components by a proper choice of a selective treatment method. The first option leads to a sludge or solid waste that is subsequently reused (if possible), landfilled (if necessary after solidification/stabilization or a similar pretreatment to avoid leaching of contaminants), or incinerated in a rotating kiln furnace (hazardous waste) or a grate furnace (nonhazardous waste). The second option leads to a (treated) wastewater, which has to be reused (if possible) or discharged in surface water (direct or indirect via sewage systems) or in groundwater.

Other factors than the volume and composition that have to be taken into account for selecting a proper treatment process are similar to reverse osmosis [81,82]: legal requirements such as permits and conditions; cost of further treatment; local factors such as the proximity and size of a wastewater treatment plant, the

presence of surface water or open land, soil characteristics, and geological structure; flexibility of the disposal method in case of an expansion of the existing plant; and public acceptance.

In the mid-1990s a survey on the use of membrane techniques in the drinking water industry in the United States was conducted [83], for installations with a capacity above 25,000 gal/day (95 m3/day). Of the 137 installations 73% were RO installations for desalination of brackish water; 11% were NF installations; another 11% were electrodialysis installations; the remaining 5% were RO plants for seawater desalination. In 48% of the installations the concentrate was discharged in surface water; in 23% the concentrate was treated in a wastewater treatment plant; in 13% the concentrate was reused on the land for, for example, irrigation; in 10% the concentrate was discharged to groundwater by deep injection; and in the remaining 6% the concentrate was discharged to evaporation ponds.

2.7.2 Types of Fouling[74]

Fouling can be broadly classified into (non-) backwashable and ir(reversible). Backwashable fouling can be removed by backwashing (reversing the direction of permeate flow through the pores of the membrane) at the end of each filtration cycle. Nonbackwashable fouling is that fouling that cannot be removed by normal hydraulic backwashing in between filtration cycles. In nonbackwashable fouling, the membrane can be returned to its original flux by other means (e.g., chemical cleaning). Irreversible fouling is that kind of fouling that cannot be removed with flushing, backwashing, chemical cleaning, or any other means, and the membrane cannot be restored to its original flux.

Inorganic Fouling/Scaling Fouling can also be classified according to the type of fouling material. Four categories of membrane fouling are generally recognized. They are: (a) inorganic fouling/scaling, (b) particle/colloidal fouling, (c) microbial/biological fouling, and (d) organic fouling. Inorganic fouling or scaling is caused by the accumulation of inorganic precipitates, such as metal hydroxides, and “scales” on membrane surface or within pore structure. Precipitates are formed when the concentration of these chemical species exceeds

their saturation concentrations. Limiting salts can be identified from solubility products of potential limiting salts in the raw feed water. Since ionic strength increases on the feed side of the membrane, the effect of ionic strength upon the solubility products should be considered. Some limiting salts can be controlled by the addition of acid or scale inhibitor or both to the feed water. Typical sparingly soluble salts that may limit recovery in pressure-driven membranes include, but are not limited to, $CaCO_3$, $CaSO_4$, $Ca_3(PO_4)_2$, $BaSO_4$, $SrSO_4$, CaF_2, and SiO_2 [U.S. Environmental Protection Agency (EPA), 2002]. Scaling is a major concern for reverse osmosis (RO) and nanofiltration (NF) since these membranes reject inorganic species. Those species form a concentrated layer in the vicinity of membrane liquid interface a phenomenon referred to as concentration polarization.

2.8 Seawater Desalination

Seawater desalination is the production of fresh, low-salinity potable or industrial-quality water from a saline water source (sea, bay, or ocean water) via membrane separation or evaporation. Over the past 30 years, desalination technology has made great strides in many arid regions of the world such as the Middle East and the Mediterranean. Today, desalination plants operate in more than 120 countries worldwide, and some desert states, such as Saudi Arabia and the United Arab Emirates, rely on desalinated water for over 70% of their water supply. According to the 2004 desalination plant inventory report prepared by the International Desalination Association (Wagnick Consulting, 2004), by the end of 2003 worldwide there were over 17,000 desalination units with total installed treatment capacity of 37.8 million m3/day. Seawater desalination plants contribute approximately 35% (13.2 million m^3/day) of this capacity[44,45,46].

Seawater is typically desalinated using two general types of water treatment technologies: thermal evaporation (distillation) and reverse osmosis (RO) membrane separation. Currently, approximately 56.5% (7.5 million m^3/day) of the world's desalination systems use RO membrane technologies. This percentage has been increasing steadily over the past 10 years due to the increasing popularity of membrane desalination, which is driven by remarkable

advances in the membrane separation and energy recovery technologies and the associated reduction of the overall water production costs. Table 2.5 presents a list of the largest seawater reverse osmosis (SWRO) desalination plants built in the last 10 years. The total capacity of these facilities is approximately 1.5 million m3/day.

Today, seawater desalination is mostly used to produce fresh potable water for human consumption and crop irrigation. Industrial applications of desalinated seawater are typically limited to its use as a low-salinity power plant boiler water, process water for oil refineries, chemical manufacturing plants, and commercial fishing installations, canneries and other food industries. The limited industrial use of seawater desalination is related mainly to the high costs associated with production of high-purity or ultrapure water from seawater. Most industrial water supply facilities use low-cost groundwater or brackish water to produce high industrial-grade water for their specific applications.

Table 2.5 Large SWRO Plants Constructed from 1996 to 2005[44,45,46]

Plant Name/Location	Capacity (m3/day)	In Operation Since
Ashkelon/Israel	325,000	2005
Tuas/Singapore	136,000	2005
Cartagena–Mauricia/Spain	65,000	2004
Fujairah/UAE	170,000	2003
Tampa Bay/United States	95,000	2003
Alikante/Spain	50,000	2003
Carboneras–Almeria/Spain	120,000	2003
Point Lisas/Trinidad	110,000	2002
Larnaca/Cyprus	54,000	2001
Al Jubail III/Saudi Arabia	91,000	2000
Muricia/Spain	65,000	1999
Bay of Palma/Palma de Mallorca	63,000	1998
Dhekelia/Cyprus	40,000	1997
Marbella–Mallaga/Spain	55,000	1997
Okinawa/Japan	40,000	1996

[a]This table includes only seawater RO desalination plants with a capacity of 40,000m3/day or higher.

2.9 Adsorption and desorption of Nitrogen Gas

BET theory is a rule for the physical adsorption of gas molecules on a solid surface and serves as the basis for an important analysis technique for the measurement of the specific surface area of a material. In 1938, Stephen

Brunauer, Paul Hugh Emmett, and Edward Teller published an article about the BET theory in a journal for the first time; “BET” consists of the first initials of their family names.

The concept of the theory is an extension of the Langmuir theory, which is a theory for monolayer molecular adsorption, to multilayer adsorption with the following hypotheses: (a) gas molecules physically adsorb on a solid in layers infinitely; (b) there is no interaction between each adsorption layer; and (c) the Langmuir theory can be applied to each layer. The resulting BET equation is expressed by (9):

$$\frac{1}{v\left[(P_0/P)-1\right]} = \frac{c-1}{v_m c}\left(\frac{P}{P_0}\right) + \frac{1}{v_m c} \tag{9}$$

P and P_0 are the equilibrium and the saturation pressure of adsorbates at the temperature of adsorption, v is the adsorbed gas quantity (for example, in volume units), and vm is the monolayer adsorbed gas quantity. c is the BET constant, which is expressed by (10):

$$c = \exp\left(\frac{E_1 - E_L}{RT}\right) \tag{10}$$

E_1 is the heat of adsorption for the first layer, and EL is that for the second and higher layers and is equal to the heat of liquefaction.

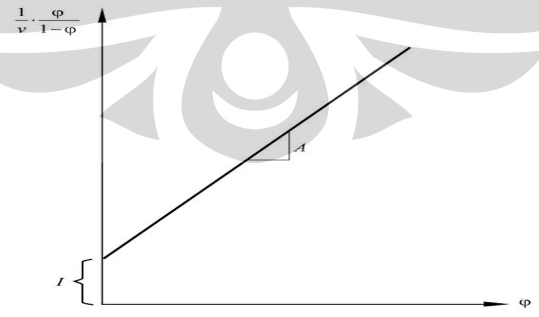

Figure 2.11 Adsorption isotherm

Equation (9) is an adsorption isotherm and can be plotted as a straight line with 1 / v[(P_0 / P) − 1] on the y-axis and φ = P / P_0 on the x-axis according to experimental results (Figure 2.11). This plot is called a BET plot. The linear

relationship of this equation is maintained only in the range of 0.05 < P / P0 < 0.35. The value of the slope A and the y-intercept I of the line are used to calculate the monolayer adsorbed gas quantity vm and the BET constant c. The following equations can be used:

$$v_m = \frac{1}{A + I} \tag{11}$$

$$c = 1 + \frac{A}{I} \tag{12}$$

The BET method is widely used in surface science for the calculation of surface areas of solids by physical adsorption of gas molecules. A total surface area Stotal and a specific surface area S are evaluated by the following equations:

$$S_{BET,total} = \frac{(v_m N s)}{V} \tag{13}$$

$$S_{BET} = \frac{S_{total}}{a} \tag{14}$$

N: Avogadro's number,
s: adsorption cross section,
V: molar volume of adsorbent gas
a: molar weight of adsorbed species

By application of the BET theory it is possible to determine the inner surface of hardened cement paste. If the quantity of adsorbed water vapor is measured at different levels of relative humidity a BET plot is obtained. From the slope A and y-intersection I on the plot it is possible to calculate vm and the BET constant c. In case of cement paste hardened in water (T=97°C), the slope of the line is A = 24.20 and the y-intersection I = 0.33; from this follows

$$v_m = \frac{1}{A + I} = 0.0408 g/g \tag{15}$$

From this the specific BET surface area SBET can be calculated by use of the above mentioned equation (one water molecule covers s = 0.114nm^2). It follows thus S_{BET} = 156m^2 / g which means that hardened cement paste has an inner surface of 156 square meters per g of cement.

For example, activated carbon, which is a strong adsorbate and usually has an adsorption cross section s of 0.16 nm^2 for nitrogen adsorption at liquid nitrogen temperature, is revealed from experimental data to have a large surface area around 3000 m² g^{-1}. Moreover, in the field of solid catalysis, the surface area of catalysts is an important factor in catalytic activity. Porous inorganic materials such as mesoporous silica and layer clay minerals have high surface areas of several hundred m² g-1 calculated by the BET method, indicating the possibility of application for efficient catalytic materials.

CHAPTER 3
EXPERIMENTAL PROCEDURE

Approach of combining of the two polymer biodegradable and non biodegradable will improve the mechanical strength and physical properties of composite membrane. Polymer biodegradable used in this study was CA and non biodegradable was PS. CA was obtained by esterification reaction of Bacterial cellulose (BC) of pineapple waste. In order to improve the membrane pores, surfactants were utilized as a pore agent.

3.1 Materials

CA (Mw average 30,000, acetyl content 43.99% similar to substitution degree of 2.8 to 2.9, 34.06% moisture content, and 148.33% yield) was produced by BC from pineapple waste formed by *Acetobater xylinum* were mercerized in NaOH 1% (w/v). The dried BC powder were acetylated with acetic acid anhydride (1:5) (cellulose:anhydride) for 2 hours. Polystyrene from Chemical Industry Indonesia and Polyethylene glycol (PEG200) from Sigma. Sodium chloride and dichloromethane both were purchased from Merck and Acetone as a solution was from Sigma. Sodium dodecyl sulphate (SDS), cetyle three methyl ammonium bromide (CTAB) and pluronic F127 from Merck were used as anionic, cationic and nonionic surfactant for addition in the casting solution. Distilled water was used through out this study.

3.2 Preparation of CA-PS membranes

Homogenous solution of CA dissolved in dichloromethane was prepared using polystyrene as invariable additive, PEG 200 and surfactants as variant additive by ultrasonic process for 16 h at room temperature. The solution then was left for 4 h to allow complete release the bubbles. The solution was sprinkled and cast on glass plate substrate and moved to the deionized water bath for immersion precipitation. The immersion process was conducted at room temperature. After primarily phase separation and formation of membrane, in order to guarantee

complete phase separation, the membrane was stored in water for 24 h. This allows the water soluble components in the membrane to be leached out. As the final stage, the membrane was dried by placing between two sheets of filter paper for 24 h at room temperature. The composition of casting solution is shown in Table 3.1.

Table 3.1 Compositions of CA/PS casting solution

CA (ml)	PS(ml)	DCM/Aceton	PEG(ml)	SDS (ml)	CTAB (ml)	Pluronic F127 (ml)
9	1	90	0	-	-	-
9	1	89.5	0.5	-	-	-
9	1	89	1	-	-	-
9	1	88.5	1.5	-	-	-
9	1	88	2	-	-	-
9	1	89.5	-	0.5	-	-
9	1	89	-	1	-	-
9	1	88.5	-	1.5	-	-
9	1	88	-	2	-	-
9	1	89.5	-	-	0.5	-
9	1	89	-	-	1	-
9	1	88.5	-	-	1.5	-
9	1	88	-	-	2	-
9	1	89.5	-	-	-	0.5
9	1	89	-	-	-	1
9	1	88.5	-	-	-	1.5
9	1	88	-	-	-	2

3.3 Characterization of CA-PS membranes

The cross section morphology of membranes was imaged by scanning electron microscopy (SEM) used Phillips scanning microscopes. The samples of membrane were frozen in liquid nitrogen and fractured. After sputtering with gold, they were viewed with the microscope at 20 kV.

Atomic force microscopy (AFM) was employed to analyze the roughness and surface morphology of membranes. The AFM apparatus included Dual Scope scanning probe optical microscope (DME model C21, Denmark). Small squares of prepared membranes (approximately 1 cm^2) were cut and glued on the glass substrate. The membrane surfaces were imaged in a scan size of 1μm x 1μm and 2μm x 2μm. Average pore sizes of membranes were obtained from height profile of AFM images using SPM software. Size of each randomly chosen pore was calculated from the information related to the height profile and pore entrance.

The stress-strain relationships were measured with a material testing machine. FTIR Spectrometer was used to investigate the blending process of CA-PS and the residual surfactants in the membrane. Nitrogen adsorption and DSC testing were investigated for supporting data.

3.4 Flux and rejection

The performance of the membrane was characterized using cross-flow system. This laboratory scale system includes reservoir, a pump, valves, pressure regulation and UF/NF cell. The rentetate was re-circulated to the reservoir and permeate was collected and weighted. The cross-flow cell house flat sheet membrane coupons with an effective area of 34 cm^2. The NaCl solution and sea water were employed as a feed for membrane performance and fouling evaluation. Each membrane was compressed with pure water at 20 psi for 1h and then the flux water was calculated by the following equation:

$$J = \frac{V}{A\Delta t}$$

For all liquid filtration studies, the results given are an average of four membranes. All values are represented as percent rejection (%R) of solute as determined by the following equation:

$$\%R = \left(1 - \frac{Cp}{Cf}\right) \times 100\ \%$$

where Cp is the concentration of the solute in the permeate and Cf is the concentration of the solute in the feed stream.

CHAPTER 4
RESULT AND DISCUSSION

4.1 Membrane characterization

Polymers for membrane preparation can be classified into natural and synthetic ones. Polysaccharides and rubbers are important examples of natural membrane materials, but only cellulose derivatives are still used in large scale for technical membranes. By far the majority of current membranes are made from synthetic polymers (which, however, originally had been developed for many other engineering applications). Macromolecular structure is crucial for membrane barrier and other properties; main factors include the chemical structure of the chain segments, molar mass (chain length), chain flexibility as well as intra- and intermolecular interactions [(24)].

Macromolecule chain flexibility is affected by the chemical structure of the main chain and the side groups. A macromolecule is flexible when unhindered rotation around single bonds in the main chain is possible. This flexibility can be reduced by several means, for example, by introducing double bonds or aromatic rings in the main chain, by forming ladder structures along the main chain or by incorporation of bulky side groups. Even larger effects with respect to the possible macroconformations can be imparted by changes of the chain architecture, that is, the transition from linear to branched or network structures [(36)]. Polymer molar mass and its polydispersity have an influence on chemical and physical properties via the interactions between chain segments (of different or even the same molecule), through noncovalent binding or entanglement. For stability, high molar mass is desirable because the number of interaction sites increases with increasing chain length. However, the solubility will decrease with increasing molar mass.

The CA-PS membranes have distinct advantages such as superior hydrophilicity, high antifouling property, and low price [(34)]. However, their permeation performance and salt rejection property are often unsatisfactory. PS is a polymer additive was function in mechanical property of membrane to increase strengthener's membrane. The preceding structural characteristics of polymer PS will strongly affect mechanical strength, thermal stability, chemical resistance and transport properties. In most polymeric membranes, the polymer is in an

amorphous state. However, some polymers, especially those with flexible chains of regular chemical structure (e.g., polyethylene (PE), polypropylene (PP) or polystyrene (PS)), tend to form crystalline domains. This will lead to higher mechanical stability (high elastic modulus) as well as higher temperature and chemical resistance than for the same polymer in amorphous state, but the free volume (and hence permeability) will be much smaller. For semicrystalline polymers, the melting temperature (Tm) is important, because at this temperature a transition between crystalline and liquid state will occur. The glass transition temperature (Tg) is a much more important parameter to characterize amorphous polymers, because at this temperature a transition between solid (glass) and supercooled melt (rubber) takes place. In the glassy state molecules are frozen, therefore, chain mobility of a polymer is very limited. Polymer selection will be more important for membranes with nonporous selective barrier, because flux and selectivity depend on the solution-diffusion mechanism. For membranes with a porous selective barrier, the mechanical stability will be crucial to preserve the shape and size of the pores [36,42,70].

Chemical or physical blending of the polymer is applied in order to control membrane swelling, especially for separations of organic mixtures. In addition, this can also enhance mechanical strength as well as chemical stability of a membrane. However, crosslinking decreases polymer solubility, therefore it is often done after membrane formation. The hydrophilicity–hydrophobicity balance of the membrane polymer is another important parameter that is mainly influenced by the functional groups of the polymer. Hydrophilic polymers have high affinity to water, and therefore they are suited as a material for nonporous membranes that should have a high permeability and selectivity for water (e.g., in RO or NF). In addition, hydrophilic membranes have been proven to be less prone to fouling in aqueous systems than hydrophobic materials [34,42].

The addition of surfactants in the casting solution can influence the membrane morphology and structure. For hydrophilic coagulant, hydrophilic surfactant is able to improve the formation of macrovoids and the hydrophilicity of membranes. However lipophilic surfactant does not have these properties. On the other hand for a lipophilic coagulant, lipophilic surfactants are more effective

in changing the membrane structure [49]. In addition, surfactants with negative or positive charge may slightly change the membrane surface charge due to their charges. This results in altering the membrane performance. In this work, the effects of anionic, cationic and non-ionic surfactant concentrations on the membrane morphology, pure water flux and sea water permeation have been investigated.

4.2. Effect of SDS as anionic surfactant on morphology and performance of CA/PS membrane

To investigate the effect of anionic surfactant as additive in the casting solution, sodium dodecyl sulphate (SDS) was selected as strong anionic surfactant. Figure 4.1 shows the effect of SDS concentration on pure water flux for prepared membrane. The pure water flux increases gradually by increasing the SDS concentration in the casting solution, reaches to a maximum at 1.5 wt% and decreases afterwards.

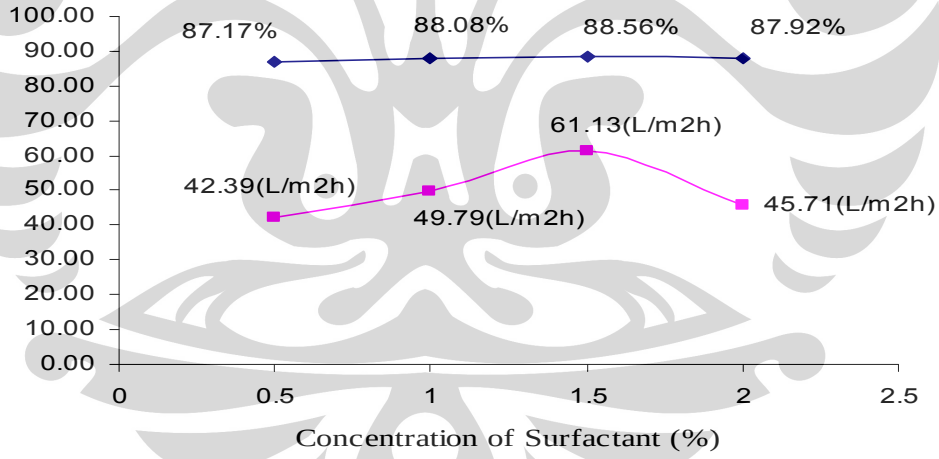

Figure 4.1 Pure water flux and salt rejection ratios of CA/PS membranes as a function of SDS content

Rejection Ratio (%)

Pure Water Flux (L/m^{2}h)

The effects of SDS concentration on sea water rejection are shown in Fig. 4.2. The obtained results demonstrate that the addition of SDS in the casting

solution enhances the seawater permeation due to the fouling process in the membrane. In the other hand, the salt rejection for prepared membranes (Fig. 4.2) shows that the salt separation increased with an increase in SDS concentration.

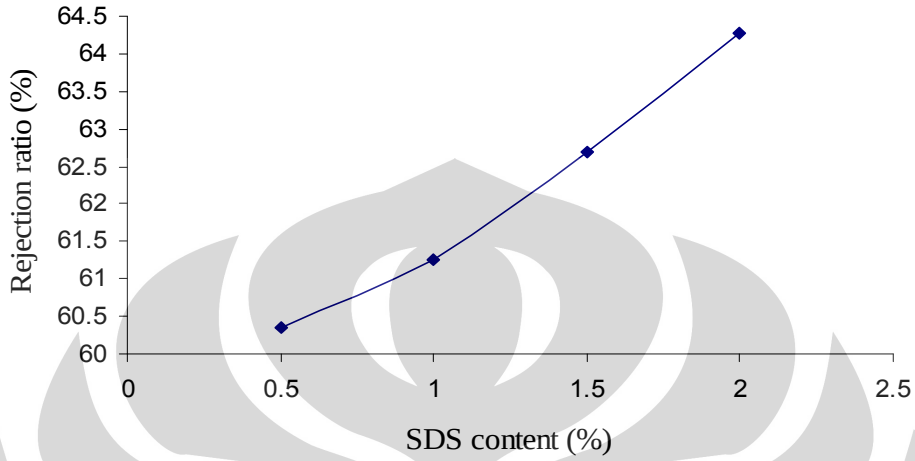

Figure 4.2 Sea water rejection ratios as a function of SDS content

The SEM images of the cross-sections of membranes prepared with different concentrations of SDS in the casting solution are shown in Fig. 4.3. The SEM images indicate that addition of small amount of SDS in the casting solution can incite macrovoids formation. The high porosity of sub-layer of membranes prepared from different concentration of SDS as additive in the casting solution, especially at 1 and 1.5 wt% of SDS, can be responsible for high performance (higher flux) of membranes.

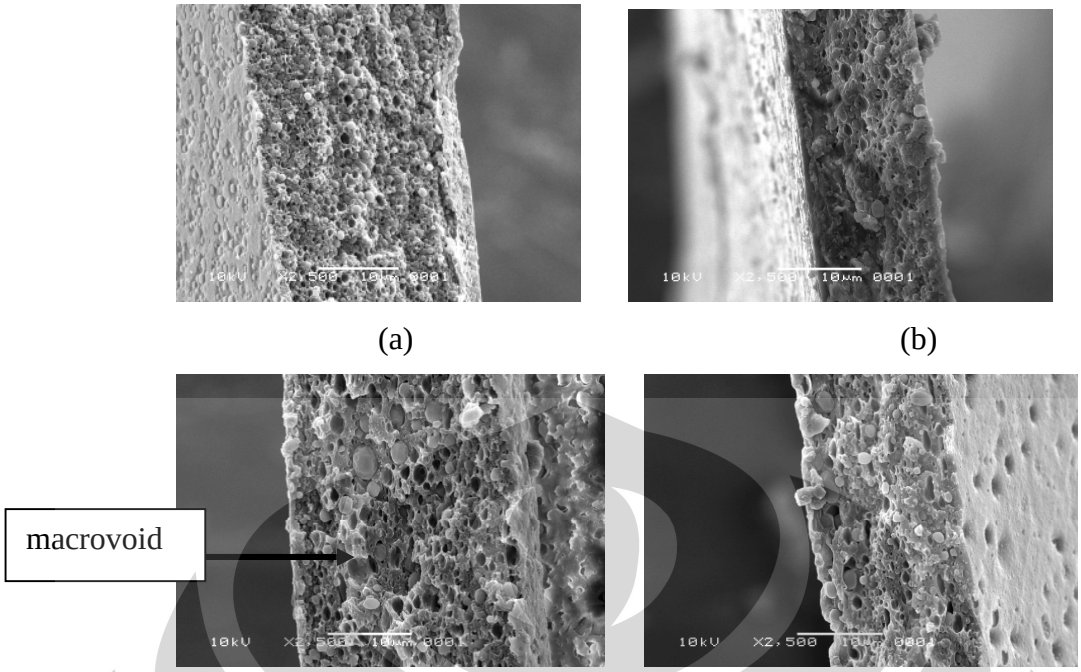

Figure 4.3 Cross-sectional SEM morphology of membranes (a) MCPS0.5 (b)MCPS1 (c) MCPS1.5 and (d) MCPS2

The addition of SDS surfactant in the casting solution may have two effects on the membrane formation processes as shown schematically in Fig. 4.4: (1) a decline of the solvent evaporation rate and (2) a diminish of interaction between polymer chain due to formation of polymer-surfactant complex [50].

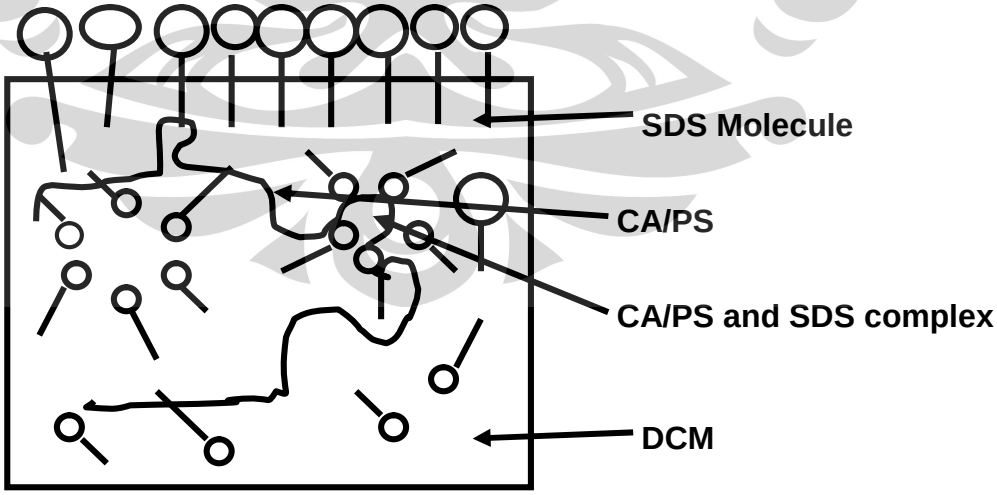

Figure 4.4 The effect of SDS on the formation of CA/PS membrane by phase inversion.

SDS is amphiphilic (i.e. with hydrophilic head and hydrophobic tail) and DCM (solvent) is hydrophobic and therefore a layer of SDS molecules is formed on the surface of the casting film [50]. This layer decreases the rate of solvent evaporation leading to slower growth of the highly concentrated polymer in the casting film. The SDS molecules and CA/PS are likely to form a micelle-like complex in the solution. The formation of this complex reduces the interaction between the polymer chains. Both phenomena result in a delay in the coagulation of polymer in the presence of SDS. Consequently the growth of skin layer is diminished and formation of sponges-like pores in the support is improved. When the concentration of SDS in the casting solution is 0.5, 1 and 1.5 wt%, all or most of SDS molecules can form a CA/PS–SDS complex. For the case of 2 wt% SDS in the casting solution, some of SDS molecules form CA/PS–SDS complex. The extra SDS establishes free micelles in the solvent phase (without formation of CA/PS–SDS complex). These free micelles corrupt the pores and leave defects in the membrane structure. The exact mechanism of formation of defects that formed in membrane surface is unknown. Its considered that some of these free micelles are located in polymer chain and also, have freely motivation in polymer chain. When the casting solution film immersed in coagulant, the free micelles leave the polymer chain, and the large pores which so called defects are formed in membrane surface. This decreases the water permeation and salt rejection.

4.3 Effect of CTAB as cationic surfactant on morphology and performance of CA/PS membrane

Cetyle three methyl ammonium bromide (CTAB) was selected for studying the effect of cationic surfactant on membrane morphology and performance. To obtain homogeneous solution, the temperature was raised to 50°C at 15 min for casting solution when CTAB was added as additive. It is clear that the temperature of casting solution influences the membrane structure and performance. Since the solubility of CTAB in DCM is very low, formation of homogeneous was done at 50°C for 15 min in casting solution. After formation of homogeneous CA/PS/DCM casting solution, CTAB was added into the homogeneous solution. After 2 h, a 50°C temperature was used to form

homogeneous CA/PS/CTAB/DCM casting solution at 15 min. The membrane structure may not be influenced due to low temperature and short time.

The effect of CTAB concentration on morphology of membranes prepared from CA/PS/DCM/CTAB system is shown in Figure 4.5. The SEM images indicate that large pores are formed in the sub-layer of membranes prepared with addition of different concentrations of CTAB in the casting solution. This phenomenon can be explained by the miscibility between the added surfactant and coagulant. However, the low solubility (or small miscibility) of CTAB in the DCM, may be introduced as another factor for changing the membrane morphology and performance. However, the author believe that the pronounced factor influencing membrane structure and forming sponge-like pores is the high miscibility between CTAB and non-solvent (up to 200 g/l).

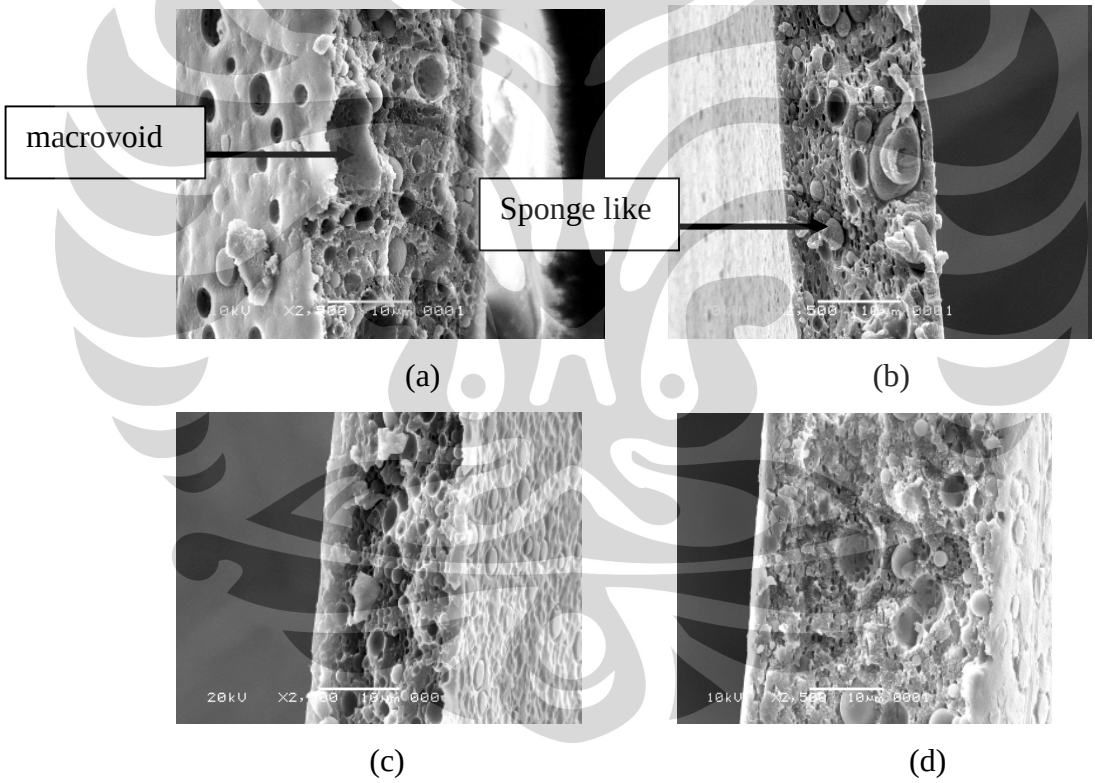

Figure 4.5 Cross-sectional SEM morphology of membranes (a) MCPT0.5 (b)MCPT1 (c) MCPT1.5 and (d) MCPT2

The miscibility between surfactant and coagulant plays an important role in the formation process of various pores. The macrovoids and sponge-like pores in the sub-layer can be induced or suppressed by addition of appropriate surfactant, depending on their miscibility with the coagulant. The addition of

surfactants that have high miscibility with the coagulant may be able to extend the formation of sponge-like pores and macrovoids. On the other hand, addition of surfactant with low miscibility with coagulant suppresses the macrovoids formation. Since the nonsolvent used in this work was the mixture of DCM (50 %) and acetone (50%), the high miscibility between CTAB as surfactant and coagulant is evident. The miscibility of CTAB in acetone is higher than 200 g/l. Thus, it is reasonable to expect that the addition of CTAB as surfactant in the casting solution induces and extends the formation of macrovoids and sponge-like pores in the support layer of membranes.

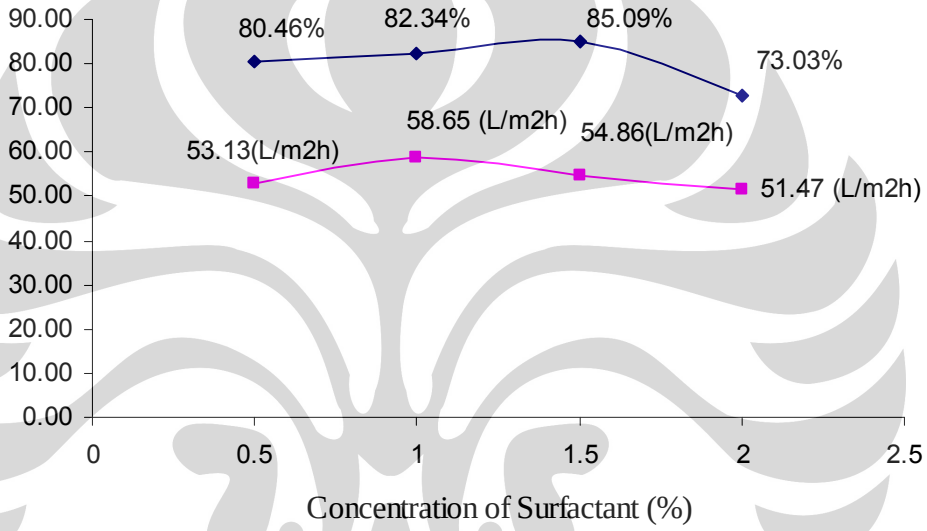

Figure 4.6 Pure water flux and salt rejection ratios of CA/PS membranes as a function of CTAB content

Rejection Ratio (%)

Pure Water Flux (L/m^{2}h)

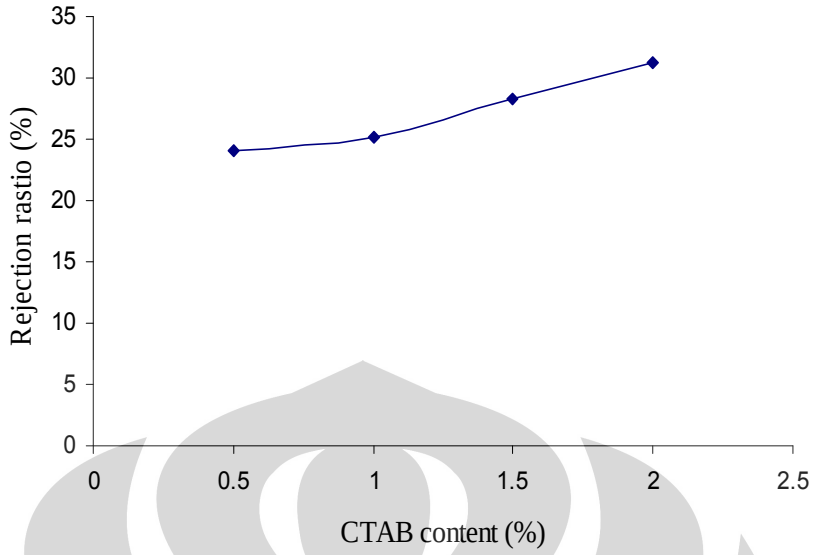

Figure 4.7 Sea water rejection ratios as a function of CTAB content

Figures 4.6 and 4.7 exhibit the effect of addition of CTAB in the casting solution on pure water flux, seawater permeation and salt rejection. These figures represent that the addition of CTAB in the casting solution result in an increase in the pure water flux and sea water permeation. Enhancement of pure water flux and seawater permeation can be explained by results obtained in Figure 4.5. The addition of CTAB in the casting solution increases the porosity of membrane support layer and results in higher pure water flux and seawater permeation.

4.4 Effect of Pluronic F127 as non-ionic surfactant on morphology and performance of CA-PS membrane

Pluronic F127 was used as non-ionic surfactant in the casting solution. The cross-sections of the membranes prepared from CA/PS/DCM/Pluronic F127 are shown in Figure 4.8.

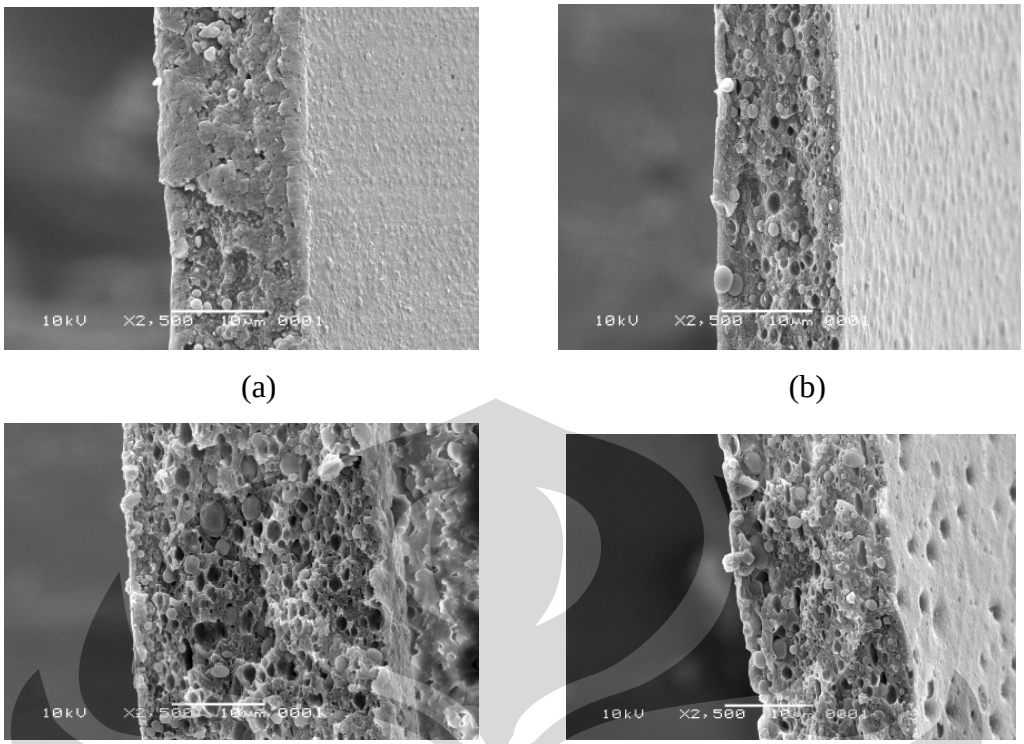

(a) (b)

(c) (d)

Figure 4.8 Cross-sectional SEM morphology of membranes (a) MCPPl0.5 (b)MCPPl1 (c) MCPPl1.5 and (d) MCPPl2

The SEM images of membranes prepared from different concentration of pluronic F127 exhibited the typical asymmetric structure and fully developed sponge-like pores in the sub-layer which are larger than pores exist in membrane prepared without pluronic F127 [(34)]. Asymmetric structure of membranes consists of a dense top layer, a porous sub-layer that is occupied by closed cell within polymer matrix, and sponge-like pores. Membranes prepared from 0.5, 1, 1.5 and 2 wt% of pluronic F127 do not represent strong changes on morphology in the sub-layer. However, there is significant difference between cross-sectional morphology of membranes prepared from CA/PS and CA/PS/Pluronic F127 systems. The presence of pluronic F127 as additive in the casting solution causes the formation of large sponge-like pores in the sub-layer of membranes.

The effect of pluronic F127concentration as additive in the casting solution on pure water flux, sea water permeation and salt rejection are shown in Figures 4.9 and 4.10, respectively.

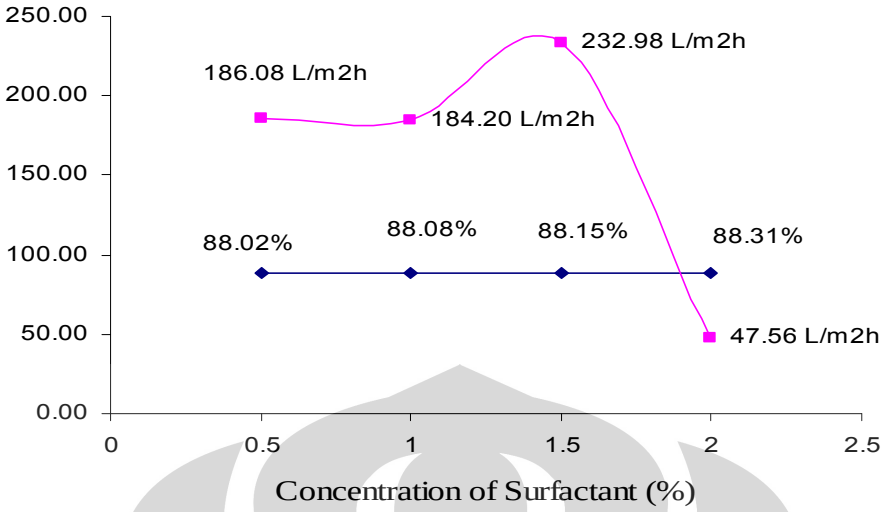

Figure 4.9 Pure water flux and salt rejection ratios of CA/PS membranes as a function of Pluronic F127 content

Rejection Ratio (%)

Pure Water Flux (L/m^{2}h)

These figures exhibited the effect of pluronic F127 as a nonionic surfactant. The pure water flux in the existing of pluronic F127 0.5% (186.07 L/m^{2}h) increases to 232.98 L/m^2 h at 1.5 wt% pluronic F127 in the casting solution and decrease dramatically at 2 wt% pluronic F127. Contrast, the seawater permeation increases as long as increased addition of pluronic concentration in the casting solution.

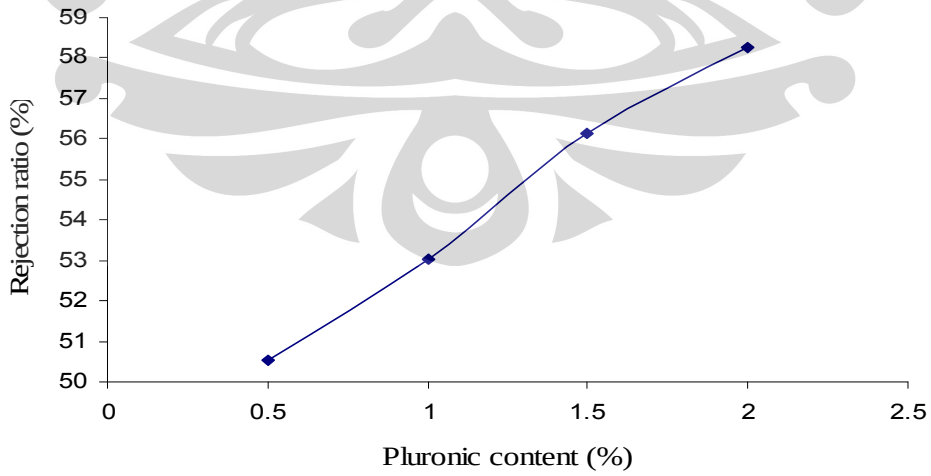

Figure 4.10 Sea water rejection ratios as a function of Pluronic F127 content

The cross-sectional morphologies of the prepared membranes the Figure 4.8 justify the high pure water flux and sea water permeation in the presence of pluronic F127 due to the porous structure of membranes.

4.5 Analysis of the surface image obtained by AFM

AFM provides essential information about the submicron surface topography and fundamental material properties of commercial or experimental membranes. Such information has been correlated with the performance (flux and solute rejection) of RO/UF/NF membranes, permeation and selectivity of gas separation membranes, and fouling potentials of membranes. Such information is, therefore, critical in optimizing the functions of membranes and designing novel antifouling surfaces. The AFM is an excellent tool for examining the topography of polymer membrane surfaces in air-dried as well as fully hydrated form (under water also). AFM provides quantitative, three-dimensional images and surface measurements with a spatial resolution of a few micrometers down to a few angstroms [(54)].

Important membrane surface properties include the size of nodules and nodule aggregates, the shape of pores, the pore size and pore size distribution, and the surface roughness. AFM seems most suitable for those. Moreover, there is evidence that nodular structure has some relationship to membrane performance. Figure 4.11 exhibited the membrane image with SDS effluent in the casting solution. From these AFM images, it seems all surfaces have relatively uniform nodular structures. However, the average diameter of the nodule aggregate at the bottom surface is 137.5 nm, which is all as large as the average diameter at the top surface (63.8 nm). The properties of the solvent in the casting solution affect the surface morphology of the membrane.

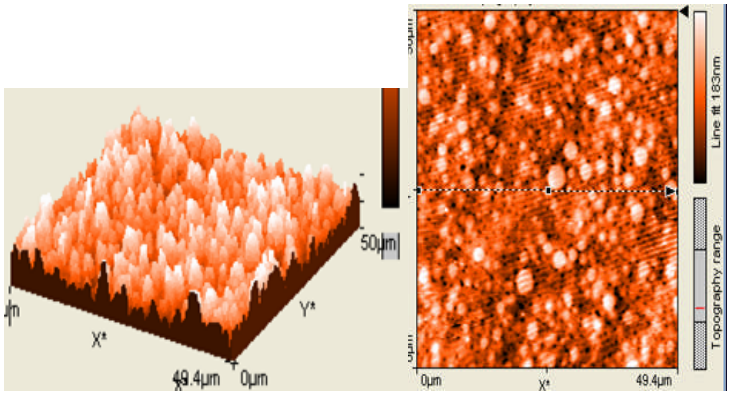

(a) MCPS0.5

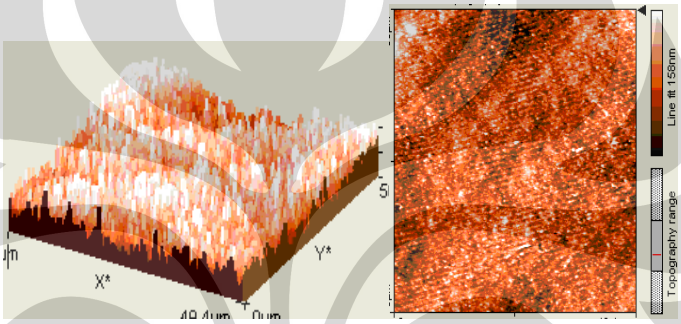

(b) MCPS1

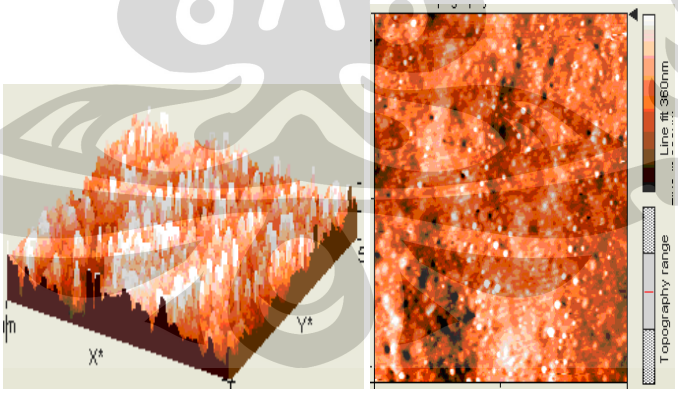

(c) MCPS1,5

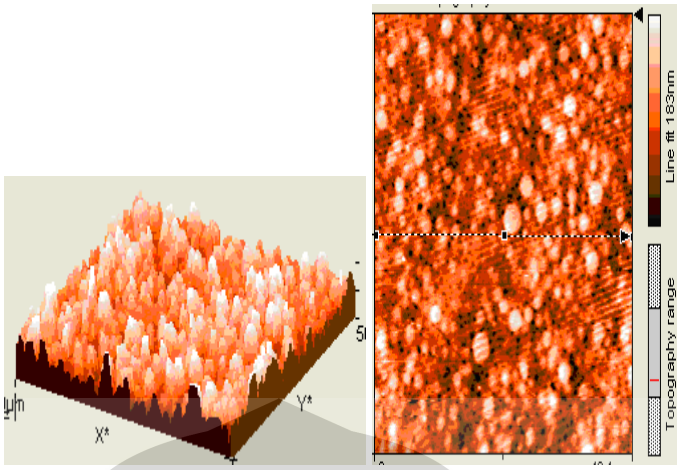

(d) MCPS2

Figure 4.11 Two and three dimensional AFM surface images of membranes (a) MCPS0.5; (b) MCPS1; (c) MCPS1.5; and (d) MCPS2.

Based on the AFM images, according to Zhang et al(2002)[51]. explained the following [51]:

- When a cast film is immersed in a coagulation bath, the casting solution at the surface that is in contact with the coagulation media will split into two phases, i.e. polymer-poor phase and polymer-rich phase [52]. After solidification, the polymer-poor phase will become pores, while the polymer-rich phase will form a polymer matrix [53]. It is believed that the solidification of cellulose acetate is more rapid when the temperature of the coagulation bath is higher due to higher diffusion rates of DCM and water. Accordingly, for a higher temperature of the coagulation bath, demixing occurs throughout the polymer solution instantly during the rapid solidification process. Therefore, the polymer is solidified before the merging of the polymer-rich phase, and larger pores are formed in comparison with those of the membranes prepared from the coagulation bath with a lower temperature.

Figure 4.11a shows a typical pore structure of a MCPS0.5 membrane in which large pores exist throughout the whole membrane surface. On the other hand, Figure 4.11b shows a nodular structure with interconnected cavity channels between the agglomerated nodules for a MCPS0.5 membrane. It is believed that

the cellulose acetate concentration affects the chain entanglement. A higher cellulose acetate concentration results in a membrane with a smaller pore size, lower flux, and higher solute rejection.

As shown in Figure 4.12 , the CA/PS membrane prepared with CTAB surfactant exhibited relatively large pores in selected surface area and the formation of nodules on membrane surface was approximately reduced. It seems that the surface pore density of this membrane is very low.

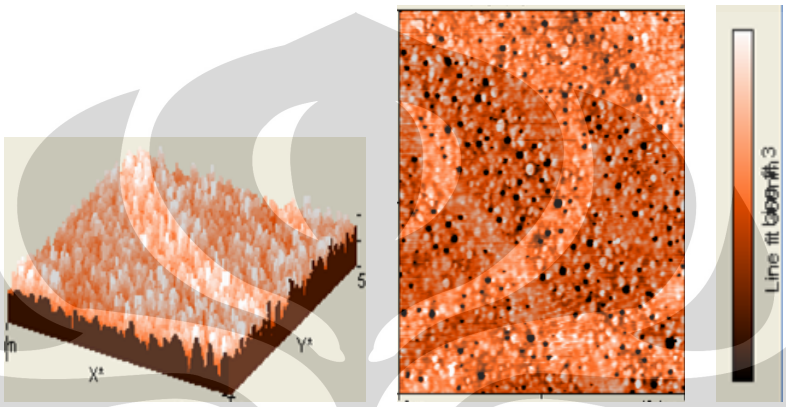

(a)MCPT0.5

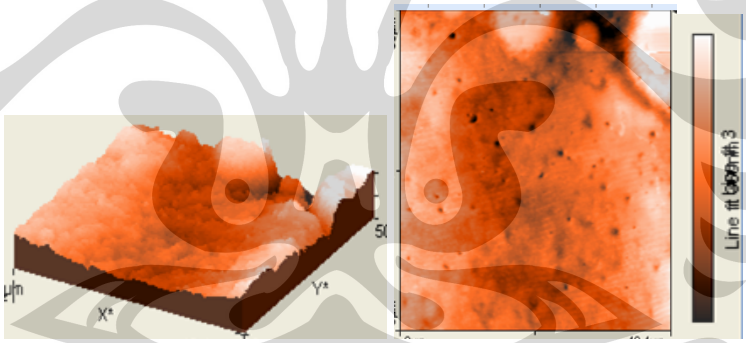

(b)MCPT1

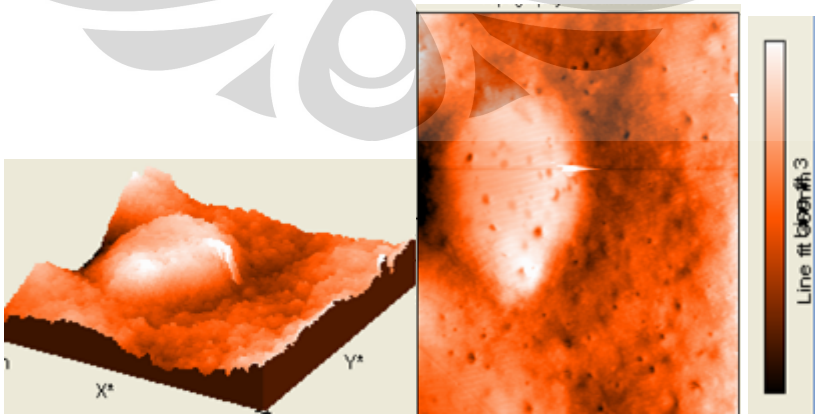

(c)MCPT1.5

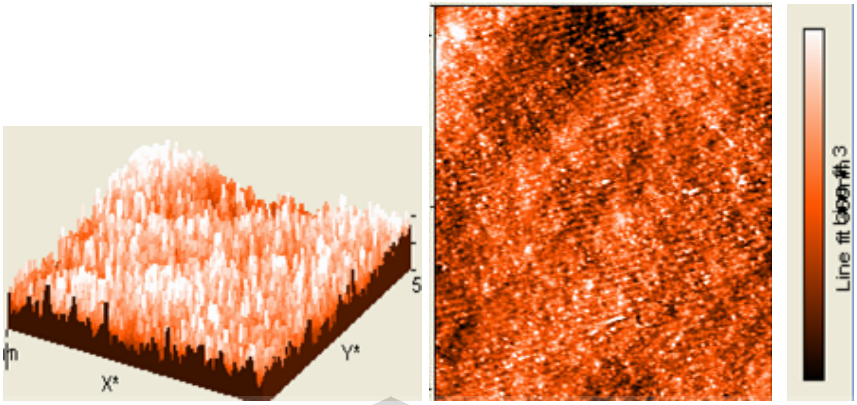

(d) MCPT2

Figure 4.12 Two and three dimensional AFM surface images of membranes (a) MCPT0.5; (b) MCPT1; (c) MCPT1.5; and (d) MCPT2.

The CA/PS membranes prepared from 0.5 wt% of SDS and CTAB demonstrated similar surface morphology with a rough and mottled surface consisting of well defined depression pores and channels. At higher concentrations of CTAB, the force was repulsive, with the appropriate decay length for charged and hydrophilic surfaces. The force was consistent with a degree of counterion binding for surface-adsorbed surfactant (2%). This result was used to infer that the surfactant aggregated into a bilayer [(63)], consisting of an inner layer of surfactant with head groups facing the CA/PS and an outer layer with head groups facing the solvent. The same evidence also supports the existence of spherical or cylindrical micelles.

Also it can be found from Figure 4.13 that the membrane with typical nodular structure and interconnected cavity channels is formed when pluronic F127 is used as surfactant in the casting solution. It seems clear that the pore density of this membrane is higher than those made from CTAB, SDS and without surfactant. Average pore size of membranes was obtained from height profile of AFM images using SPM software.

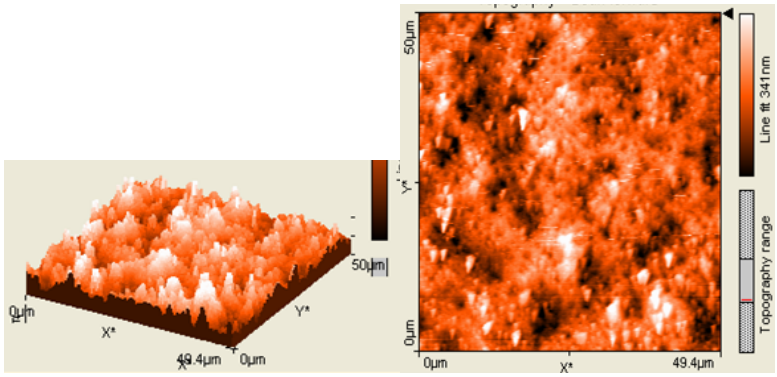

(a) MCPPl 0.5

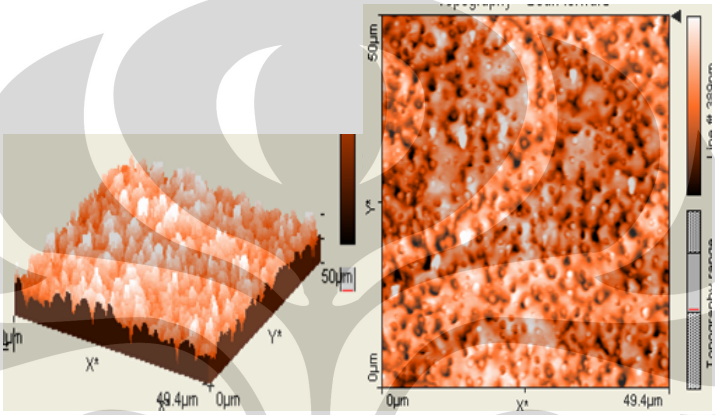

(b) MCPPl1

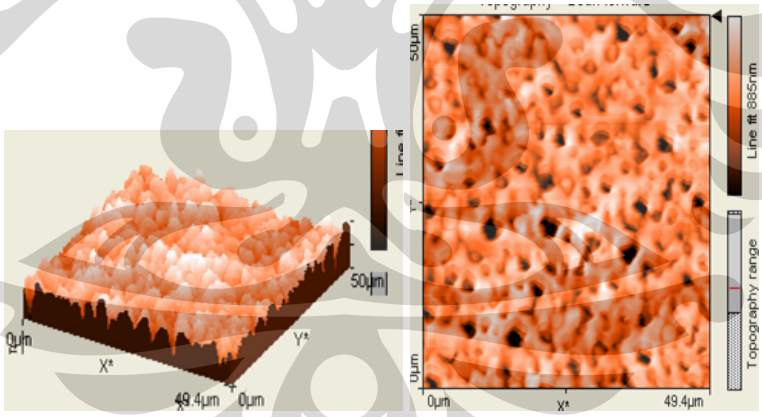

(c) MCPPl1.5

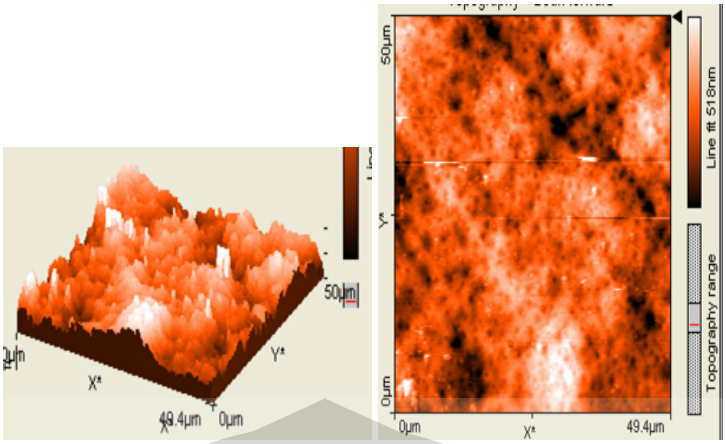

(d) MCPPl2

Figure 4.13 Two and three dimensional AFM surface images of membranes (a) MCPPl0.5; (b) MCPPl1; (c) MCPPl1.5; and (d) MCPPl2.

Since the membrane surface porosity prepared with different surfactants is approximately alike, the membrane with lower pore size has lower pure water flux. It means that pluronic F127 membrane exhibits lower pure water flux compared to SDS and CTAB membranes. The lower seawater flux of pluronic F127 membrane may be explained due to the fouling mechanism [78]. For the membranes with small pores in the top layer, the particles form a layer on the membrane surface. However for the membranes with large pores, the particles enter into the membrane structure and entrap within the pores. These results in blockage of the pores providing extra resistance against the passage of sea water through the membrane i.e. lower flux. The surface roughness parameters of the membranes which are explained in terms of the mean roughness (*Sa*), the root mean square of the *Z* data (*Sq*) and the mean difference between the highest peaks and lowest valleys (*Sz*) were calculated by SPM DME software. The obtained results are presented in Table 4.1

Table 4.1 Surface roughness parameters of different membranes obtained from AFM images

Membrane	Sa	Sq	Sz
MCPT0,5	0,410 μm	0,470 μm	2.500μm
MCPT1	1,200 μm	1,400 μm	5.500μm
MCPT1,5	0,910 μm	1,000 μm	3.800μm
MCPT2	1,300μm	1,500 μm	4.600μm
MCPPl0,5	0.050 μm	0.064 μm	0.540 μm
MCPPl1	0.099 μm	0.120 μm	0.930 μm
MCPPl1,5	0.260 μm	0.310 μm	2.090 μm
MCPPl2	0.210 μm	0.250 μm	1.500 μm

This table indicates that the membrane roughness parameters increase with addition of surfactants in the CA/PS casting solution. Moreover when pluronic F127 is used as additive, the membrane roughness is smaller compared to the other surfactants. Although Fritzche et al. [54] and Bessieres et al. [55] observed the direct correlation between membrane surface roughness and molecular weight cut-off (MWCO), but comparing Tables 4.1 indicate that the MWCO of the membranes is reduced with addition of surfactant in the CA/PS casting solution. This behavior may be due to the surfactant properties. Most surfactants have a long hydrophobic alkali and a hydrophilic ionic group (polar group) in their structure. When the surfactant molecule enters in aqueous media the ionic head tends to water while the non-polar tail tends to move away and leave from water. Therefore, the surfactant tends to absorb on solid surface, air or organic phase. The alkali chain can join to polymer matrix when it comes near to hydro-carbonic structure of polymer but the hydrophilic and polar portion leave freely. The accumulation of polar groups in polymer structure results in repulsion between polymer chains and consequently increases the porosity of membrane by forming an open structure. When the surfactant concentration increases, the non-polar tail of surfactant molecules settle beside one another and form micelles with polar groups in outer surface and non-polar groups inside the micelles in addition to the polymer surfactant complex. These free micelles deteriorate the membrane

structure and decrease the membrane performance. In most cases, the performance of membrane still is better than the membranes made without surfactant [50]. The difference between performances of membranes prepared from SDS and CTAB may be due to difference between space prevention of their polar head. The SDS has polar head with higher space prevention compared to CTAB. This leads to higher interaction between polymer and SDS and consequently the membrane performance slightly decrease. The performance of membranes prepared from pluronic F127 is higher compared to those prepared from SDS and CTAB. Pluronic F127 is a non-ionic compound and has massive structure and may link to polymer structure via its functional groups. Under this circumstance, an open configuration in the polymer chains is formed resulting in higher flux for the membranes.

A dense homogeneous cellulose acetate membrane was exhibited by figures 4.11; 4.12 and 4.13. On comparing Figs. 4.12 b. and 4.12c, it seems that the nodule aggregates have swollen by wetting and are fused with each other, forming larger nodular aggregates. This is reflected by the increases observed in the nodule size and the roughness parameter. Interestingly, there is only little change, both in the figures and in the data shown in Table 4.1, when the water-wet surface is dried at room temperature [54]. In other words, the swelling of the nodule aggregates was irreversible. Most likely, the fusion of the nodule aggregates is responsible for the high salt rejection in RO as well as high selectivity in gas separation of the cellulose acetate membrane.

Table 4.2 Performance properties and AFM parameters of membranes

Membrane Type	Salt (NaCl) rejection (%)	Pure water Permeability (L/m^2h)	Average roughness, *Sa* (nm)
MCPPL0.5	88.017	186.078	50
MCPPL1	88.077	184.201	99
MCPPl1.5	88.154	232.982	260
MCPPL2	88.313	47.563	210

Correlation concerning surface roughness and fouling was reported by Elimelech et al. [56], in which they studied the surface morphology of cellulose acetate and composite aromatic polyamide RO membranes by AFM and correlated their findings with membrane colloidal fouling. They observed higher fouling rates for the thin film composite membrane compared to those for the cellulose acetate membrane. The higher fouling rate for the thin film composite membrane was attributed to its greater value of surface roughness, which was inherent in interfacially polymerized aromatic polyamide composite membranes. AFM showed that attachment of the grafted layer onto the active surface did not lead to significant changes in the surface morphology. While a certain reduction of roughness could be obtained with RO membranes, the characteristic "hills and valleys" morphological pattern did not undergo a qualitative change, even for high degrees of grafting. Hence, grafting did not prevent the colloidal fouling of the membrane, whereas it was effective for the reduction of organic fouling.

Table 4.2 indicates that there is no correlation between the roughness parameter and the membrane data, including pure water permeability and solute separation. On the other hand, colloidal fouling of RO and NF membranes is nearly perfectly correlated with membrane surface roughness, regardless of physical and chemical operating conditions. It was further demonstrated that AFM images of fouled membranes yielded valuable insights into the mechanisms governing colloidal fouling. At the initial stages of fouling, AFM images (Fig.4.13) clearly show that more particles are deposited on the rough membranes than on the smooth membranes. Particles preferentially accumulate in the *valleys* of rough membranes, resulting in *valley clogging*, which causes more severe flux decline than in smooth membranes.

In an AFM (86), the surfactant aggregate is probed by measuring the force between a sharp tip and the micelle adsorbed at the interface between the solid and the solution. To obtain contrast there must be lateral variation in the force between the tip and the adsorbed micelle. This lateral variation in the force arises from both topography and chemical variations. The resolution is maximized in two ways: (1) by using a very sharp tip that receives a large contribution of total force from a small area of the solid and (2) by making measurements where the

force has a very high gradient normal to the surface. Sharp AFM tips typically have a radius of about 10 nm, which is similar to the smallest radius of curvature of adsorbed micelles. Therefore, the force between the tip and the micelle at any tip location includes large force contributions arising from a region of the micelle, not from a point on the micelle. Thus, AFM tips of today cannot be used to map accurately the shape of highly curved adsorbed micelles. The lateral extent of a small micelle can be estimated from an AFM image by examining the spacing between the centers of adjacent micelles. In other words, the AFM is good at examining the arrangement of micelles, which can then be used to infer the shape (4158,63,).

The adsorption of charged surfactants often results in the generation of a charge on the sample and sometimes on the tip. These charges are compensated by counterions that inhabit the solution between the tip and the sample. Some of the counterions are closely associated with the surfactant head groups and some exist in a diffuse layer in solution. As the tip approaches the sample, work is required to confine these counterions to a smaller volume and, therefore, the tip experiences a repulsive force, which is known as the electrostatic double-layer force. The gradient of this force depends on the surface charge and on the concentration of electrolyte in solution. The gradient is larger for higher concentrations of electrolyte in solution. (For example, the double-layer force in a 1:1 electrolyte has a decay length of ≤10 nm in a 1 mM solution and a decay length of ≥1 nm in a 100 mM solution.) Therefore, the resolution of AFM imaging should be greater as an electrolyte is added to the solution. Of course, the addition of electrolyte may also affect the actual structure of the adsorbed micelles. Adsorbed surfactants also generate surface forces due to the energy required to remove water from the surfactant head groups (hydration forces) and the energy required to confine the surfactant to a smaller volume on the surface (protrusion forces). These short-range forces (<1 nm) have high gradients that are ideal for AFM imaging. In contrast, the longer range double-layer force usually has a lower gradient, which decreases the resolution in the vertical direction and causes the interaction between the sides of the tip and the sample to make significant contributions to the total force. This effectively widens the tip. Therefore, it

should be easier to obtain higher solution images of net-uncharged surfactants or of charged surfactants in concentrated salt solutions [45,86].

4.6 Mechanical membranes analysis

The mechanical property of the nanofiltration membrane was another major concern for the practical application. The mechanical properties (mean values of three samples) of CA/PS membranes with different surfactants content were shown in Figure 4.14. The mechanical properties of modified CA membranes were highest with the addition of pluronic F127 1%, and decreased gradually at 1.5% pluronic F127, which might be due to the increasing porosity of the membranes. However, the modified membranes could still meet the mechanical requirements for practical nanofiltration.

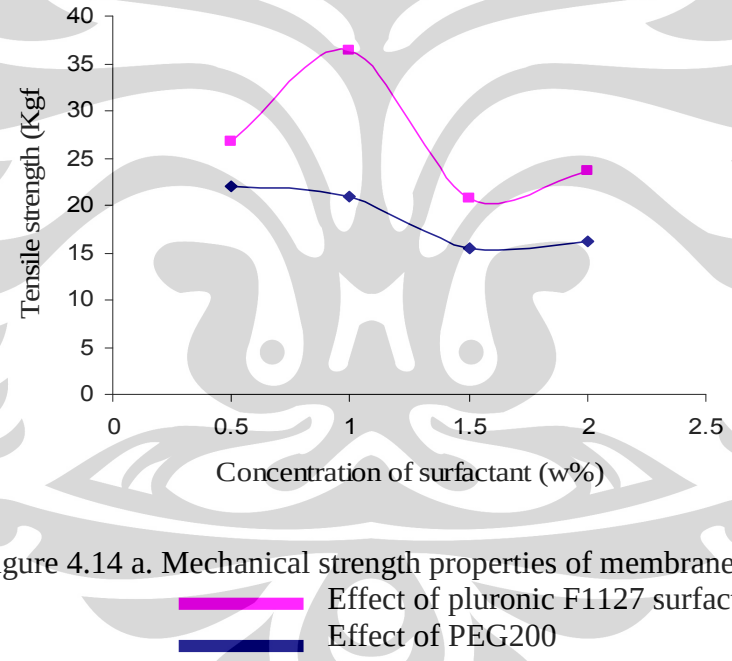

Figure 4.14 a. Mechanical strength properties of membranes

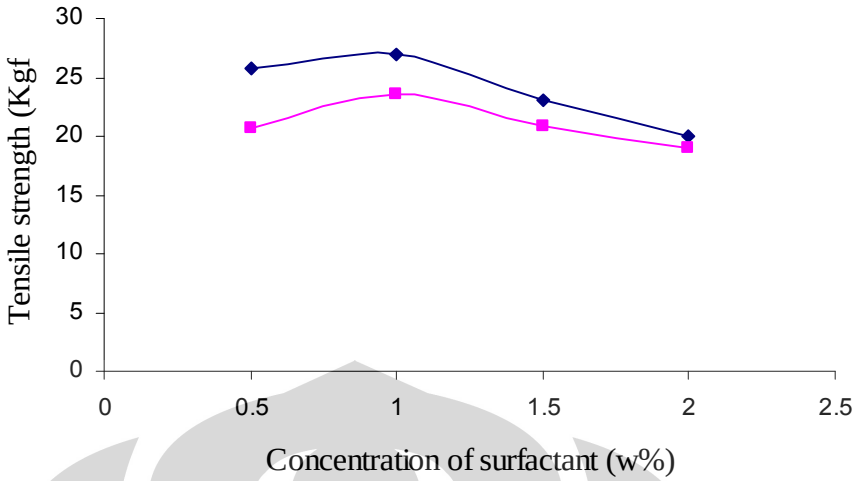

Figure 4.14 b. Mechanical strength properties of membrane
Effect of CTAB surfactant
Effect of SDS surfactant

. The hydrophilicity of modified CA membranes was increased with an increase in pluronic F127 content. That was probably due to the residual pluronic F127 on the surface of CA membranes which ensured the substantial increase in the hydrophilicty of membranes surface. Also, the addition of SDS and CTAB as a anionic and cationic surfactant in the casting solution shows decreased with the increased of surfactant addition.

4.7 Analyze of FTIR [57]

In order to obtained the quantitative information for CA-PS matrix membrane, in the current study FTIR was employed to measure of the linking between CA and PS. FTIR spectra of CA-PS membrane is shown in Fig.4.15

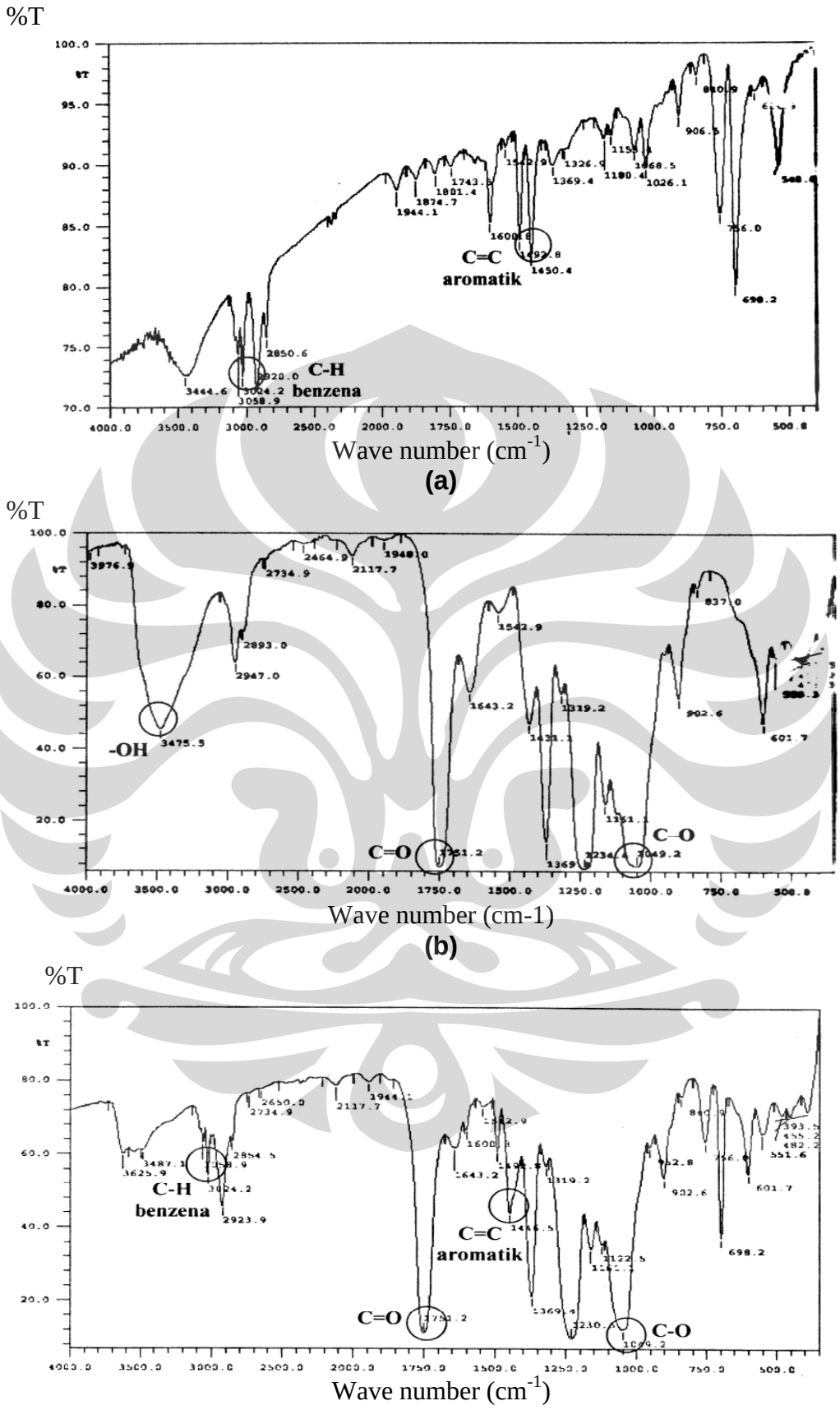

Figure 4.15 FTIR spectra of ; a. PS film; b.CA film; c. CA-PS membrane

Figure 4.15a showed spectra of CA wherein strong sorption in wave number of 1751.2 cm-1 was exhibited due to C=O ester group. This suggests that CA has acetyl group. But, there was another –OH group in 3475 cm-1, this obviously indicates that acetylating reaction of CA compound was not complete. CA had acetyl number only 43,26% or equal with substitution degree of 2.8. Due to acetyl number of CA compound, CA only dissolves in dichloromethane. Another spectrum was observed at 1049,2 cm-1 (C-O group). Availability of C=O group in CA is supported by availability of C-O group [57].

A spectrum of PS (Figure 4.15 b) has specific spectra with strong sorption in 3024.2 cm-1 and indicated C-H benzene group. The wave number 1450,4 of C=C aromatic was supported the existing benzene group. The Fig.3[c] showed spectra of CA-PS Specific peaks of sorption at CA and PS both exhibited the composite membrane CA-PS. Spectra showed of C=O ester group in wave number 1751.2 cm-1 and C-O group in wave number 1049.2 cm-1. This indicated the specific spectra for CA. Similar was the case of PS wherein specific spectra is exhibited in the Figure 3[c]. Sorption peak in wave number 3024.2 cm-1 for C-H benzene group and 1446.5 cm-1 for C=C aromatic group. Composite membrane CA-PS was not obtaining new compound and not reaction happened between CA and PS. Matrix membrane were built by matrix linking between CA and PS.

It was shown in Figure 4.16 (a) that a considerable change in the FTIR spectra of the CA/PS films appeared after incorporation of the pluronic F127: the peak at 2870 cm^{-1} assigned to symmetric C-H stretching vibration of methylene groups of the mixed films was higher than that of the CA/PS film. This increase was due to the contribution of CH_2 group from pluronic F127. The relative intensity of 2870 cm^{-1} peak was gradually enhanced with an increase of pluronic F127 content in the mixed films.

Similarly, spectrum FTIR of membrane MCPS and MCPT shows (Fig.4.16b and 4.16c), the specific function groups were contained by SDS and CTAB only appeared in the SDS and CTAB spectrum not in the membrane spectrum, which indicated that most of the added surfactants have been leached out from CA/PS membranes into coagulation bath.

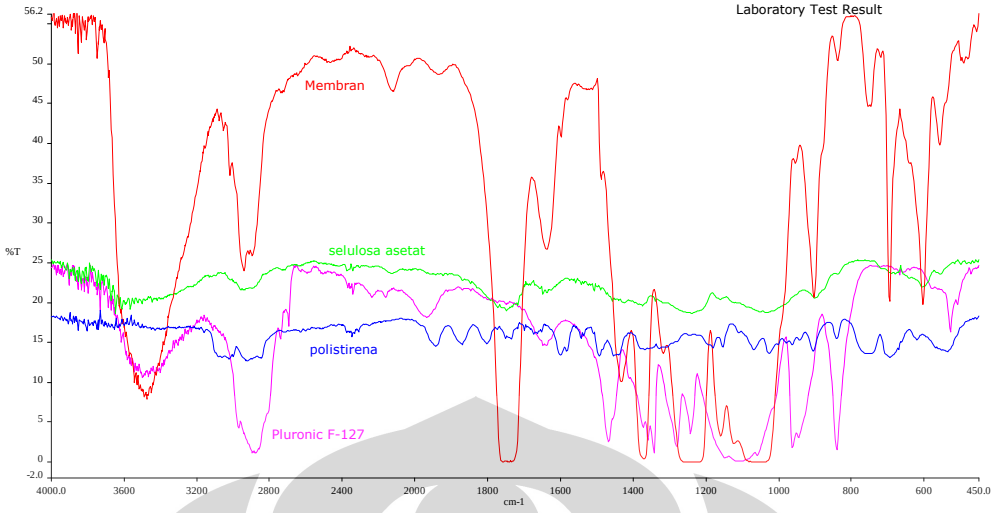

(a)

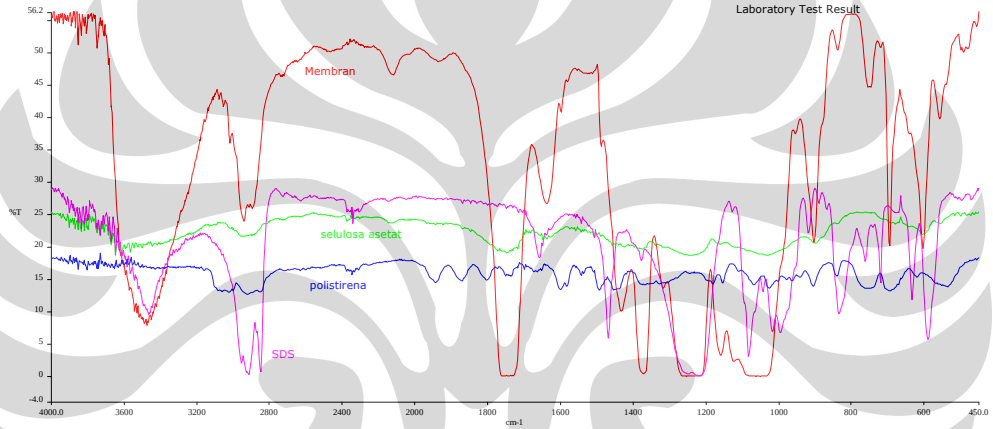

(b)

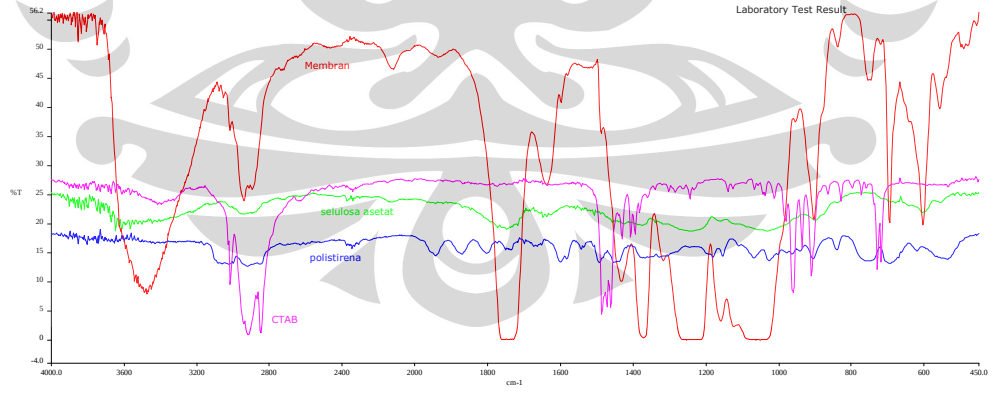

(c)

Figure 4.16 (a) Spectrum FTIR membrane MCPPl, PS,CA and pluronic F127
(b) Spectrum FTIR membrane MCPS, PS, CA and SDS
(c) Spectrum FTIR membrane MCPT, PS, CA and CTAB

4.8 Effect of surfactant in the membranes pore

Surfactants (anionic, cationic and nonionic) can be able to affect the membranes pores. Generally, when an aromatic molecule (CA/PS) is intercalated between the head groups or the long-chain hydrophobic of the surfactant in the micelles, the chemical shifts for some of the protons of the surfactant monomers are up field because of the effect of the current of the aromatic ring [58]. The results obtained in this study clearly show the complexity of the size and shape of surfactant micelles in DCM/Acetone solution with the addition of CA/PS. A small amount of surfactant solubilized in the interfacial region of the aggregates renders rod like micelles larger and longer. As a result of this process, the viscosity of the dilute surfactant systems will rise and the viscoelasticity of concentrated solutions will increase due to the formation of a network structure of the micelles. When the CTAB content is higher, it will be solubilized in the palisades of the micelles and the rod like micelles transform gradually into smaller oblate spheroid ones. Both the viscosity of dilute surfactant systems and the viscoelasticity of concentrated micellar systems will decrease. Regarding to this phenomena, the pore membrane influenced by CTAB has much larger pores compare with pluronic and SDS.

The many uses of surfactants have stimulated research on surfactant adsorption and on surfactant aggregation in bulk solution. For some time, evidence has suggested that surfactants also aggregate in the adsorbed state. The ability of the AFM to obtain these images has allowed researcher to examine the relationship between intermolecular forces and the shape of the adsorbed micelle. The concept of surface aggregation for surfactants was first introduced to explain abrupt changes in interfacial properties as a function of surfactant concentration. Fritzche *et al*. (54) inferred the existence of surface aggregates from zeta potential measurements, which showed an increase in the gradient of surfactant adsorption at a particular concentration. This concentration was approximately a constant fraction of the critical micelle concentration (cmc), which suggested that the surface process was similar to bulk micellization. Unlike simple monovalent ions, surfactant ions reversed the charge of solids even when they were not lattice ions. This adsorption against an electrostatic potential implied that the surfactants attracted each other. In early work, the attractive force was assumed to be van der

Waals interactions, but later it was attributed to the hydrophobic effect. The surface density and wetting properties of the surfactant clusters were consistent with the surfactant adopting an orientation with the alkyl chains facing the solution. These small clusters were called ‘‘hemimicelles.’’

At the surface of a liquid the coordination of a molecule is reduced. The creation of a surface therefore requires an input of energy. The situation is complicated by two factors. First, a molecule at the surface also gains entropy from its greater freedom of movement and hence the surface free energy, which is what is most easily measured (Figure 4.17), is very different from the surface energy. Secondly, the surface energy is measured per unit area, not per mole. The surface layer of molecules will adjust their coordination to optimize the gain in entropy and the loss in energy. This has an average layer intermediate in density between bulk and vapour, and the coordination of a molecule in this surface layer is much less than half its value in the bulk [59a].

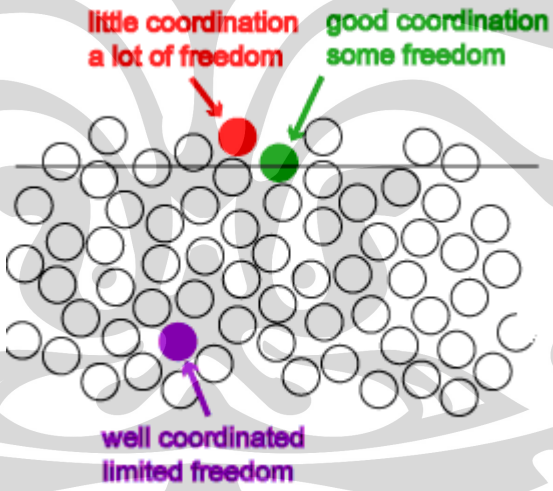

Figure 4.17 Schematic of surfactants phenomenon in solubilization

From this study can represent the situation a bit more clearly by drawing immiscible species, squares and circles, as Figure 4.18. Solubilization of polymer CA/PS with surfactants (SDS, CTAB and Pluronic F127) in the DMC/Acetone emphasize on the amphiphilic beahviour that can be generated by joining two chemical groupings with opposite solubility characteristics. An amphiphile will attempt to remove its hydrophobic part from the aqueous environment while keeping its hydrophilic part in water. One way it can achieve this situation by self-

aggregation, e.g. the molecules can align themselves to form aggregates with the hydrophobic tails [88].

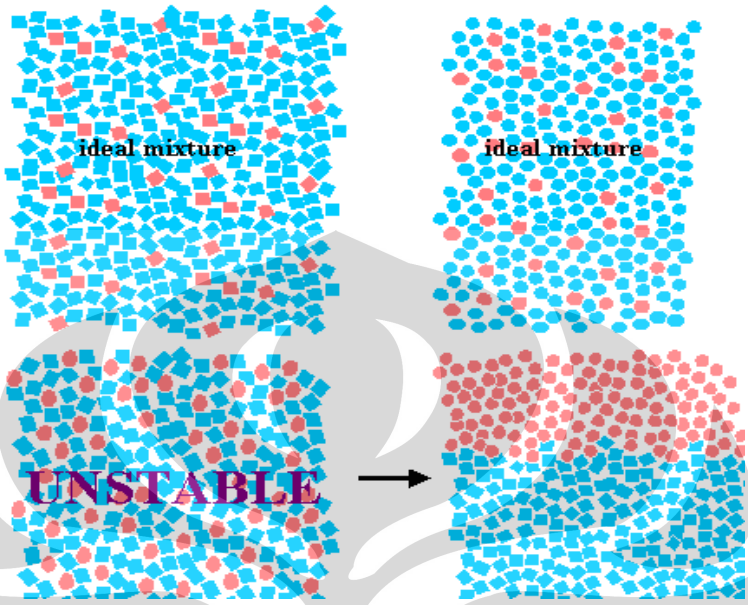

Figure 4.18 Solubilization of CA/PS with surfactant

The soluble amphiphilic molecules self-assemble into aggregates in solution can be demonstrated experimentally in many ways. Measurement of almost any physical property of the solution shows a discontinuity in the physical property at a particular concentration, which is characteristic of the compound being examined at the chosen temperature. The discontinuity is usually associated with the formation of micelles and is known as the critical micelle concentration (CMC) [84]. However, the study conducted on addition surfactant above CMC level, the experimental evidence for the shape and size of the aggregates that are formed is less easy to obtain. The aggregates are too small to be directly observable by light scattering (that is why the solutions usually appear quite clear). The most direct method is by x-ray or neutron scattering. A typical micelle has a radius about equal to the fully extended length of the chain of the surfactant molecule, i.e. about 20 Å, and contains of the order of 100 molecules.

It is useful to be able to assess to what extent the nature of the aggregates can be manipulated by changing the molecular geometry. There are three easily manipulated factors, (i) the design of the initial molecule, i.e. choosing values of v, a, and l, (ii) varying a using the external conditions, e.g. adding electrolyte to

reduce electrostatic repulsion between the head groups, (iii) by adding a third component. Addition of electrolyte to a solution of a charged electrolyte above its CMC always acts to reduce and hence induce spherical micelles to become rod-like. This behaviour is easily followed because rods get entangled with each other and the solution goes very viscous. It is this effect of added electrolyte that is the dominant factor in the idealized sequence of phases shown by a surfactant solution as the concentration of surfactant is increased [88] .

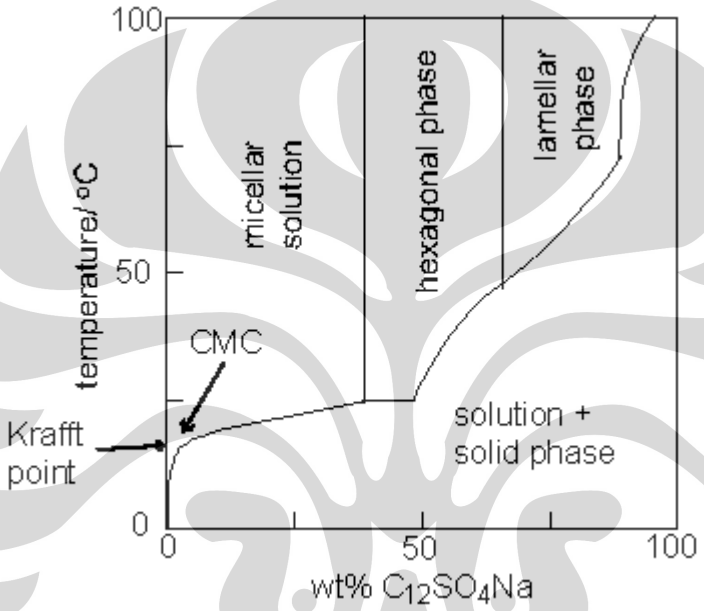

Figure 4.19 Effect of temperature towards surfactants

The addition of a third component can be used in two ways. If a non-polar material is added it will prefer to occupy the interior of the micelle and, if it is fluid, it will assist the packing of the ends of the surfactant chain. It will therefore be incorporated into the micelle (solubilization) and this is one of the factors that contribute to detergent action [88]. However, there is a limit to how much material can be solubilised because swelling of the micelle will cause the surface of the micelle to be defective and hence allow water to come into contact with the interior. The maximum size of particle that is thermodynamically stable is achieved by modifying the surfactant layer by increasing v/al, either by changing the structure of the surfactant molecule or by adding a co-surfactant.The maximum size in a thermodynamically stable system is a radius of about 5 nm.

Such solutions are called microemulsions. Ordinary emulsions, which have much larger particle sizes, are not thermodynamically stable.

Deviation from the Langmuir adsorption isotherm is often used to infer the aggregation of surfactants at interfaces. The Langmuir adsorption isotherm assumes that the adsorption energy is independent of surface coverage, and deviation is used to signal the presence of concentration-dependent intermolecular forces, e.g., electrostatic forces or the hydrophobic effect. The use of deviations from idealized isotherms to indicate aggregation is somewhat problematic because two interactions can produce opposing effects. For example, electrostatic interactions and hydrophobic interactions may combine to produce adsorption that resembles the Langmuir adsorption isotherm [88].

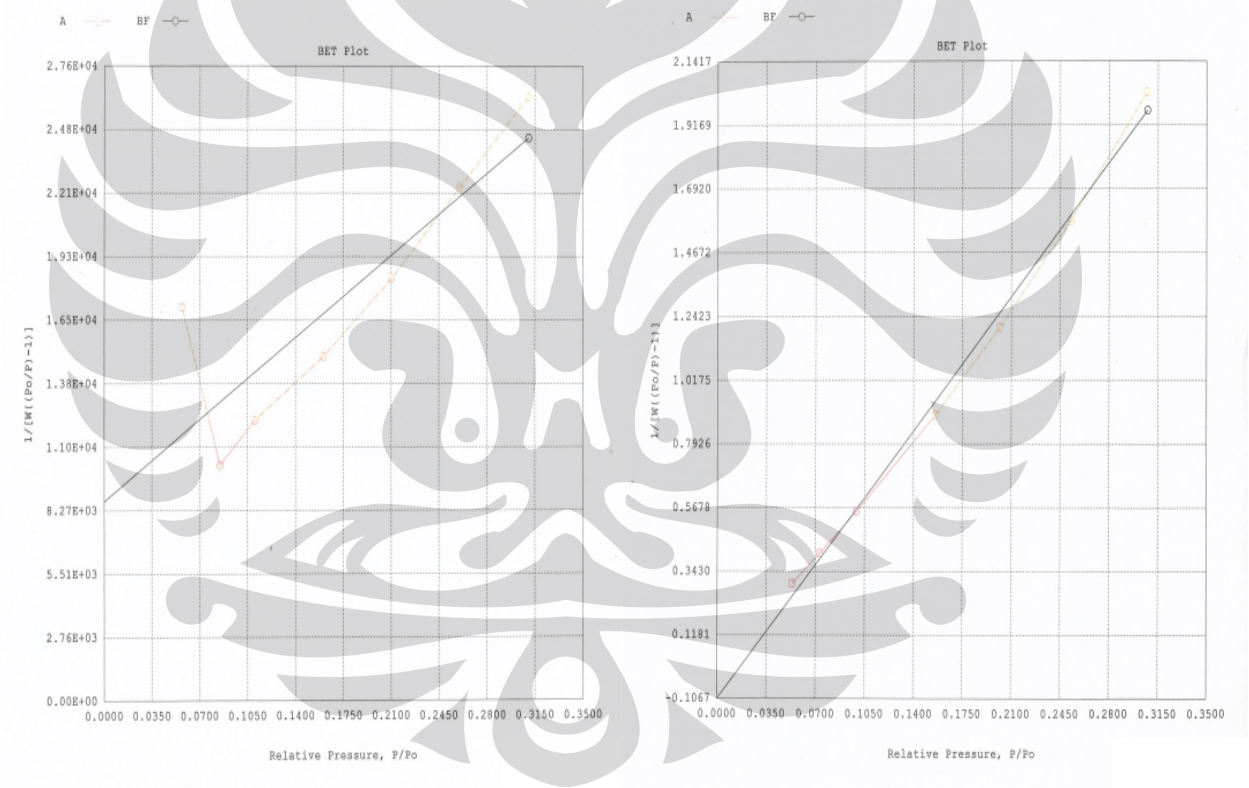

Figure 4.20 Curve of Adsorption-desorption of (a) MCPT membrane and (b) MCPPl membrane

Figure 4.20 represent the adsorption–desorption of N2 gas on the membrane surface. According to BET result, MCPPL membrane showed pore radius is 16,00 Å, and MCPT membrane was 240 nm. The surface area of membrane was obtained 15,7 m^2/g dan 785,6 m^2/g. for MCPT membrane and MCPPl membrane respectively.

4.9 Thermal Analysis of Membrane

Thermal analysis of the membrane was evaluated by *Differential Scanning Colorimetry*.

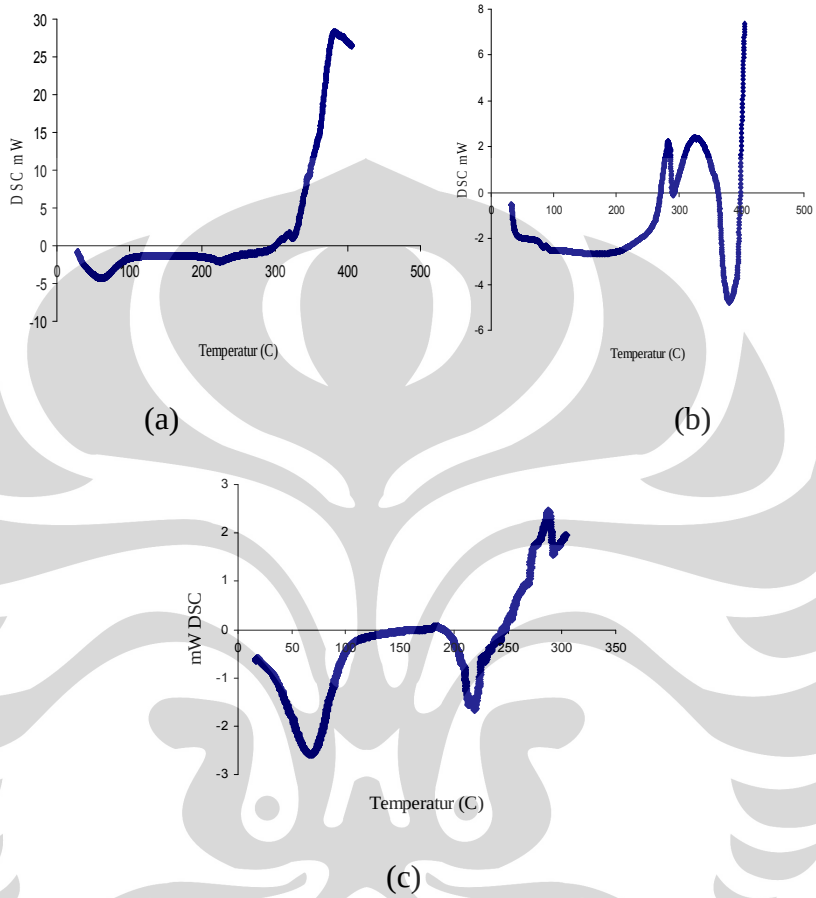

Figure 4.21 Thermogram DSC (a) CA;(b) PS; (c) membrane

Figure 4.21 exhibited thermogram of membrane content 3 of Tg (75^0C as CA amorf, 250^0C as a PS crystalline and 300^0C as a CA crystalline). The Tg indicated that membrane merely contain CA and PS polymer and there was no chemical reaction occurred in the membrane. The result has supported the FTIR data.

4.9 Comparison between effects of SDS, CTAB and Pluronic F127

Figure 4.22 shows the comparison between the effects of three surfactants on pure water permeation. This figure indicates that the pure water permeation is higher compared to two other cases when pluronic F127 is used as additive in the casting solution. In general, the addition of small amount of surfactant has strong effect on morphology and performance of CA/PS membrane.

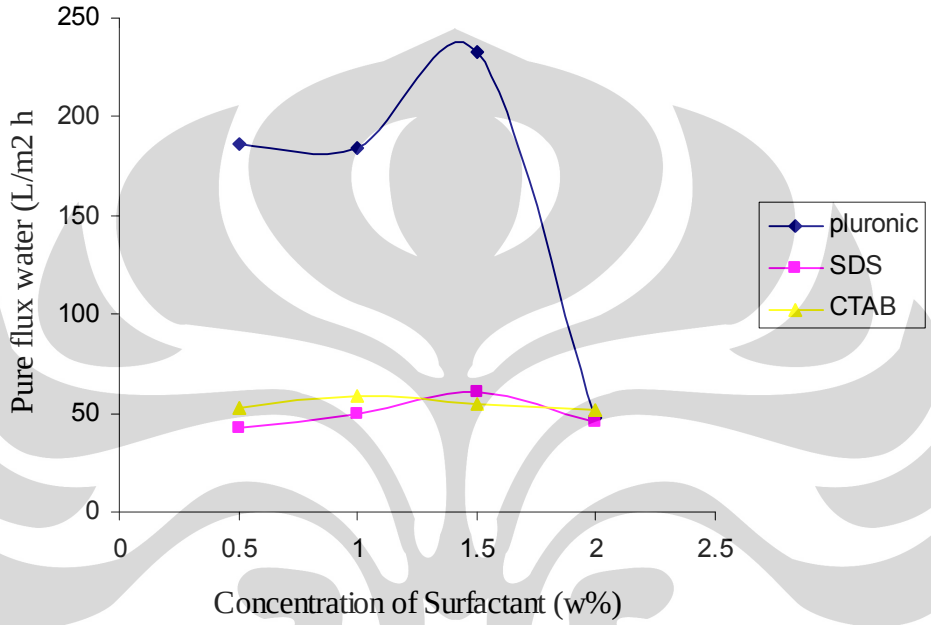

Figure 4.22 Comparison between the effects of three surfactants on pure water permeation.

In contrast, the SDS is used as additive in the casting solution sea water rejection is higher compared to two other cases of surfactant additive (CTAB and pluronic F127) (Figure 4.23). Since the membrane surface porosity prepared with different surfactants is approximately alike, the membrane with lower pore size has lower purewater flux. It means that SDS membrane exhibits lower pure water flux compared to CTAB and pluronic F127 membranes.

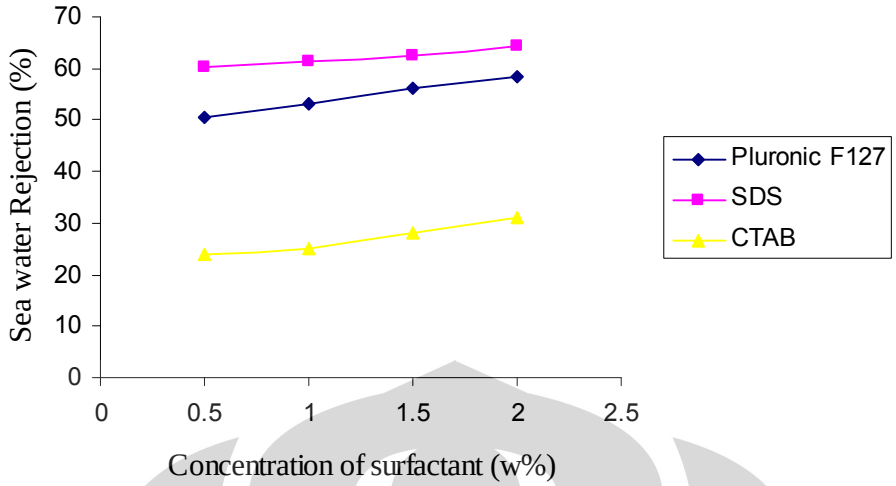

Figure 4.23 Comparison between the effects of three surfactants on sea water rejection.

The higher sea water rejection of SDS membrane may be explained due to the fouling mechanism. For the membranes with small pores in the top layer, the particles form a layer on the membrane surface. However for the membranes with large pores, the particles enter into the membrane structure and entrap within the pores. This esults in blockage of the pores providing extra resistance against the passage of sea water through the membrane, i.e. lower flux.

Most surfactants have a long hydrophobic alkali and a hydrophilic ionic group (polar group) in their structure. When the surfactant molecule enters in aqueous media the ionic head tends to water while the non-polar tail tends to move away and leave from water. Therefore, the surfactant tends to absorb on solid surface, air or organic phase. The alkali chain can join to polymer matrix when it comes near to hydro-carbonic structure of polymer but the hydrophilic and polar portion leave freely. The accumulation of polar groups in polymer structure results in repulsion between polymer chains and consequently increases the porosity of membrane by forming an open structure. When the surfactant concentration increases, the non-polar tail of surfactant molecules settle beside one another and form micelles with polar groups in outer surface and non-polar groups inside the micelles in addition to the polymer surfactant complex. These free micelles deteriorate the membrane structure and decrease the membrane

performance. In most cases, the performance of membrane still is better than the membranes made without surfactant. The difference between performances of membranes prepared from SDS and CTAB may be due to difference between space prevention of their polar head. The SDS has polar head with higher space prevention compared to CTAB. This leads to higher interaction between polymer and SDS and consequently the membrane performance slightly decrease. The performance of membranes prepared from pluronic F127 is higher compared to those prepared from SDS and CTAB. Pluronic F127 is a non-ionic compound and has massive structure. Pluronic F127 may link to polymer structure via its functional groups. Under this circumstance, an open configuration in the polymer chains is formed resulting in higher flux for the membranes.

CHAPTER 5
CONCLUSION

From the present study it can be concluded that:

1. CA-PS composite membranes can be formed from material based of Bacterial Cellulose resulted by *A.xyllinum* in the pineapple garbage juice medium. This indicated that the economically low value pineapple garbage can be utilized to produced CA composite membrane of potentially high economic value.
2. The performance of the membrane can be enhanced by using PS as additive agent and surfactant as pore forming agent.
3. It was found that the addition of small amounts of surfactants in the casting solution increases the formation of macrovoids and sponge-like pores in the sub-layer of membranes. This enhances the pure water flux and sea water permeation. When pluronic F127 was used as additive in the casting solution the performance of prepared membrane was higher compared to the other cases.
4. The FTIR measurement confirmed that majority of surfactants has been leached out from the CA membranes after immersed in aqueous coagulation bath.
5. The SEM photographs showed that the surfactants played a crucial role in modifying the structure of membranes with different porosity and pore size. Membrane MCPT has bigger pore volume compared with that in others membranes.
6. AFM supported for studying the structure of the membrane surface. Higher roughness parameters seem to enhance permeation rates of membranes.
7. Mechanical strength of membranes showed that membrane with addition of SDS and pluronic F127 in the casting solution has a higher tensile strength number than that membrane with addition of CTAB.
8. The all of the membranes can be used for water desalination process. Rejection value test showed that membrane with addition of SDS has a higher (64.27%) rejection value than that of membrane MCPT and MCPl.

REFERENCES

1. Li Lianchao ,Wang Baoguoa, Tan Huimin b, Chen Tianlu c, Xu Jiping , *A novel nanofiltration membrane prepared with PAMAM and TMC by in situ interfacial polymerization on PEK-C ultrafiltration membrane* Journal of Membrane Science 269 (2006) 84–93

2. Yanagishita H, D. Kitamoto, K. Haraya, T. Nakane, T. Tsuchiya, N. Koura, *Preparation and pervaporation performance of polyimide composite membrane by vapor deposition and polymerization (VDP)*, J. Membr. Sci. 136 (1997) 121–126

3. Yanagishita H., D. Kitamoto, K. Haraya, T. Nakane, T. Okadab, H. Matsuda, Y. Idemoto, N. Koura, *Separation performance of polyimide composite membrane prepared by dip coating process*, J. Membr. Sci. 188 (2001) 165–172.

4. Yanagishita H, J. Arai, T. Sandoh, H. Negishi, D. Kitamoto, T. Ikegami, K. Haraya, Y. Idemoto, N. Koura, *Preparation of polyimide composite membranes grafted by electron beam irradiation*, J. Membr. Sci. 232 (2004) 93–98.

5. Hayakawa Y., N. Terasawa, E. Hayashi, T. Abe, *Plasma polymerization of cyclic perfluoroamines and composite membranes for gas separation*, J. Appl. Polym. Sci. 62 (1996) 951–954

6. Zhi-Ping Zhao, Jiding Li, Dan-Xia Zhang, Cui-Xian Chen, *Nanofiltration membrane prepared from polyacrylonitrile ultrafiltration membrane by low temperature plasma*, J. Membr. Sci. 232 (2004) 1–8.

7. Ulbricht M., Hans-Hartmut Schwarz, *Novel high performance photograft composite membranes for separation of organic liquids by pervaporation*, J. Membr. Sci. 136 (1997) 25–33.

8. Zhigong R, L. Guixiang, T. Sugo, J. Okamoto, *Gas-phase and liquidphase pre-irradiation grafting of Aac onto LPPE and HDPE films for pervaporation membranes*, Radiat. Phys. Chem. 39 (5) (1993) 421.

9. Peterson J., K.-V. Peinemann, *Novel polyamide composite membranes for gas separation prepared by interfacial polycondensation*, J. Appl. Polym. Sci. 63 (1997) 1557–1563.

10. Morgan W., *Condensation Polymers: By Interfacial and Solution Methods*, Interscience, New York, 1665, pp. 19–64.

11. Anagi M. Balachandra, Gregory L. Baker1, et al., *Preparation of composite membranes by atom transfer radical polymerization initiated from a porous support*, J. Membr. Sci. 227 (2003) 1–14.

12. Guangling Pei, Guoxiang Chenga, Qiyun Du, *Preparation of chelating resin filled composite membranes, and selective adsorption of Cu(II)*, J. Membr. Sci. 196 (2002) 85–93.

11. Xu Tongwen, Yang Weihua, *A novel positively charged composite membranes for nanofiltration prepared from poly(2,6-dimethyl-1,4-phenylene oxide) by in situ amines cross-linking*, J. Membr. Sci. 215 (2003) 25–32.

12 Marshall. A.D., P.A. Munro, *The effect of protein fouling in microfiltration and ultrafiltration on permeate flux, protein retention and selectivity*: a literature review, Desalination 91 (1993) 65–108.

13. Zhifeng Fan, Zhi Wang, Meirong Duan, Jixiao Wang, Shichang Wang *Preparation and characterization of polyaniline/polysulfone nanocomposite ultrafiltration membrane* Journal of Membrane Science 310 (2008) 402–408

14. Kim S.H., S.Y. Kwak, B.-H. Sohn, T.H. Park, *Design of TiO2 nanoparticle self-assembled aromatic polyamide thin-film-composite (TFC) membrane as an approach to solve biofouling problem*, J. Membr. Sci. 211 (2003) 157–165.

15.. Bae T.H, T.M Tak., *Effect of TiO2 nanoparticles on fouling mitigation of ultrafiltration membranes for activated sludge filtration*, J. Membr. Sci. 249 (2005) 1–8.

16. Bae T.H., T.M. Tak, *Preparation of TiO2 self-assembled polymeric nanocomposite membranes and examination of their fouling mitigation effects in a membrane bioreactor system*, J. Membr. Sci. 266 (2005) 1–5.

17. Luo M.-L., J.-Q. Zhao, W. Tang, C.-S. Pu, *Hydrophilic modification of poly(ether sulfone) ultrafiltration membrane surface by self-assembly of TiO2 nanoparticles*, Appl. Surf. Sci. 249 (2005) 76–84.

18. Yan L., Y.S. Li, C.B. Xiang, *Preparation of poly(vinylidene fluoride) (PVDF) ultrafiltration membrane modified by nano-sized alumina (Al_2O_3) and its antifouling research*, Polymer 46 (2005) 7701–7706.

19. Gibson P., H. Schreuder-Gibson, D. Rivin, *Transport properties of porous membranes based on electrospun nanofibers*, Colloid Surf. A: Physicochem. Eng. Aspects 187–188 (2001) 469–481.

20. Barhate R.S., C.K. Loong, S. Ramakrishna, *Preparation and characterization of nanofibrous filtering media*, J. Membr. Sci. 283 (2006) 209–218.

21. Gopal R., S. Kaur, Z. Ma, C. Chan, S. Ramakrishna, T. Matsuura, *Electrospun nanofibrous filtration membrane*, J. Membr. Sci. 281 (2006) 581–586.

22. Gopal R., S. Kaur, C.Y. Feng, C. Chan, S. Ramakrishna, S. Tabe, T. Matsuura, *Electrospun nanofibrous polysulfone membranes as pre-filters: particulate removal*, J. Membr. Sci. 289 (2007) 210–219.

23. Yoon K., K. Kim, X. Wang, D. Fang, B.S. Hsiao, B. Chu, *High flux ultrafiltration membranes based on electrospun nanofibrous PAN scaffolds and chitosan coating*, Polymer 47 (2006) 2434–2441.

24. Wang X., D. Fang, K. Yoon, B.S. Hsiao, B. Chu, *High performance ultrafiltration composite membranes based on poly(vinyl alcohol) hydrogel coating on crosslinked nanofibrous poly(vinyl alcohol) scaffold*, J. Membr. Sci. 278 (2006) 261–268.

25. Anderson M.R., B.R. Mattes, H. Reiss, R.B. Kaner, *Conjugated polymer films for gas separations*, Science 252 (2001) 1412–1415.

26. Kuwabata S., C.R. Martin, *Investigation of the gas-transport properties of polyaniline*, J. Membr. Sci. 91 (1994) 1–12.

27. Huang S.C., I.J. Ball, R.B. Kaner, *Polyaniline membranes for pervaporation of carboxylic acids and water*, Macromolecules 31 (1998) 5456–5464.

28. Naidu B.V.K., M. Sairam, K.V.S.N. Raju, T.M. Aminabhavi, *Pervaporation separation of water isopropanol mixtures using novel nanocomposite membranes of poly(vinyl alcohol) and polyaniline*, J. Membr. Sci. 260 (2005) 142–155.

29. Wang P., K.L. Tan, E.T. Kang, K.G. Neoh, *Preparation and characterization of semi-conductive poly(vinylidene fluoride)/polyaniline blends and membranes*, Appl. Surf. Sci. 193 (2002) 36–45.

30. Kaner R.B., *Gas,liquid and enantiomeric separations using polyaniline*, Synth. Met. 125 (2002) 65–71.

31. L. Rebattet, M. Escoubes, E. Genies, M. Pineri, *Effect of doping treatment on gas transport properties and on separation factors of polyaniline membranes*, J. Appl. Polym. Sci. 57 (1995) 1595–1604.

32. Huang J., R.B. Kaner, *Nanofiber formation in the chemical polymerization of amine: a mechanistic study*, . Chem. Int. Ed. 43 (2004) 5817–5821.

33. Zhong W., X. Chen, S. Liu, Y. Wang, W. Yang, *Synthesis of highly hydrophilic polyaniline nanowires and sub-micro/nanostructured dendrites on poly(propylene) film surfaces*, Macromol. Rapid Commun. 27 (2006) 563–569.

34. Cailing Lv, Yanlei Su, Yanqiang Wang, Xiaole Ma,Qiang Sun, Zhongyi Jiang, *Enhanced permeation performance of cellulose acetate ultrafiltration membrane by incorporation of Pluronic F127*, Journal of Membrane Science 294 (2007) 68–74.

35. Altaf H. Basta , Houssni El-Saied 2008. *Enhanced transport properties and thermal stability of agro-based RO-membrane for desalination of brackish water* Journal of Membrane Science 310 (2008) 208–218

36. Turbak A.F., *Membranes from cellulose and cellulose derivatives*, Appl.Polym. Symp. 13 (1969) 61.

37 Power, Special Report Water Treatment", A McGraw-Hill Publication (June 1993).

38. Khedr M.G., Proc. IDAWorld *Congress on Desalination and Water Reuse*, Abu Dhabi, UAE, 1995.

39. Khedr M.G, *Desalination Water Reuse* 10 (3) (2000) 8.

40. Ponti M.M., et al., *Les Techniques Separatives a Membranes: Theory, Applications et Perspectives*, CEE-UIE Paris, 2001.

41. El-Saied H., *Effect of Functional groups in cellulose derivatives on permeability properties*, Master Thesis, Faculty of Science, Cairo University, Cairo, 1968.

42. Donald L., *Cellulose acetate blend membranes-useful in reverse osmosis*, IFI Appl. No. 19720524, USA, 1972.

43. Weston E.R, H.W. Heidsman, B. Keilin, U.S., 3, 250, 701 (Cl. 210-22), May 1966, Appl. September 1965.

44. Baker, R.W. *Membrane Technology and Applications*, 2nd edition, John Wiley & Sons, Ltd, Chichester, (2004)Chapters 2, 3, 5, 6 & 9.

45. Matsuura T, Norman N. Li, Anthony G. Fane, W. S. Winston Ho, *Advanced Membrane Technology and Applications* (2008) John Wiley & Sons, Inc

46. Mulder, M. Basic *Principle of Membrane Technology*, 2nd edn, Kluwer Academic Publishers, Dordrecht, (1996) Chapters 2, 3 & 5.

47. Hsieh, P. *Inorganic Membranes for Separation and Reaction*, (1996)Elsevier, Amsterdam.

48. Marcano, J.G.S. and Tsotsis, T.T. *Catalytic Membranes and Membrane Reactors*, (2002) Wiley-VCH, Weinheim.

49. D.M. Wang, F.C. Lin, T.T. Wu, J.Y. Lai, *Formation mechanism of the macrovoids induced by surfactant additives*, J. Membr. Sci. 142 (1998) 191.

50. Yamasaki A., R.K. Tyagi, A.E. Fouda, K. Jonnason, T. Matsuura, *Effect of SDS surfactant as an additive on the formation of asymmetric polysulfone membranes for gas separation*, in: I. Pinnau, B.D. Freeman (Eds.), Membrane Formation and Modification, 2000.

51. Zhang Y, Shao H, Hu X (2002) J Appl Polym Sci 86:3389

52. Cheng LP, Soh YS, Dwan A, Gryte CC (1994) J Polym Sci Part B Polym Phys 32:1413

53. Khayet M, Feng CY, Khulbe KC, Matsuura T (2002) Polymer 43:3879

54. A.K. Fritzche, A.R. Arevalo, M.D. Moor, C.J. Weber, V.B. Elings, K. Kjoller, M.C. Wu, *Image enhancement of polyethersulfone ultrafiltration membrane surface structure for atomic force microscopy*, J. Appl. Polym. Sci. 46 (1992) 167.

55. A. Bessieres, M. Meireles, R. Cortager, J. Beauvillian, V. Sanchez, *Investigations of surface properties of polymeric membranes by near field microscopy*, J. Membr. Sci. 109 (1996) 271.

56. Elimelech M, Zhu X, Childress AE, Hong S (1997) J Membr Sci 127:101

57. Pavia, D.,Garry M. Lampman, George Kriz, *Introduction to a spectroscopy*, (2001) Thomson Learning Inc. USA

58. Matsuura, T. (2001). *Progress in membrane science and technology for seawater desalination—A review*. Desalination 134, 47–54.

59. Cadotte, J.E. (1985) *Material Science of Synthetic Membranes* (ed. D.R. Lloyd), ACS Symposium Series 269, American Chemical Society, Washington DC, pp.273–294.

60. Asatekin, A., Menniti, A., Kang, S., Elimelech, M., Morgenroth, E. and Mayes, A.M. (2006) Journal of Membrane Science, 285, 81–89.

61. Rana, D., Matsuura, T. and Narbaitz, R.M.(2006) Journal of Membrane Science, 277, 177–185.

62. Scha¨fer, A. I., Fane, A. G., and Waite, T. D. (Eds.) (2005). *Nanofiltration Principles and Applications.* Elsevier, Oxford.

63. Vankelecom, I. F. J., De Smet, K., Gevers, L. E. M., and Jacobs, P. A. (2005). *Nanofiltration membrane materials and preparation*. In A. I. Schna¨fer, A. G. Fane, and T. D., Waite (Eds.), Nanofiltration—Principles and Applications. Elsevier, Oxford.

64. Siewert, C., Richter, H., Piorra, A., and Tomandl, G. (2000). *Development of ceramic nanofiltration membranes*. Ind. Cer. 20(1), 31–33.

65. Tsuru, T., Sudoh, T., Yoshioka, T., and Asaeda, M. (2001b). *Nanofiltration in non-aqueous solutions by porous silica-zirconia membranes.* J. Membr. Sci. 185(2), 253–261.

66. Voigt, I., Stahn, M., Wohner, S., Junghans, A., Rost, J., and Voigt, W. (2001). *Integrated cleaning of coloured waste water by ceramic NF membranes*. Separ. Purif. Technol. 25(1–3), 509–512.

67. Van Gestel, T., Vandecasteele, C., Buekenhoudt, A., Dotremont, C., Luyten, J., Leysen, R., Van der Bruggen, B., and Maes, G. (2002). *Alumina and titania multilayer membranes for nanofiltration: Preparation, characterization and chemical stability*. J. Membr. Sci. 207, 73–89.

68. Van der Bruggen, B., Schaep, J., Maes, W., Wilms, D., and Vandecasteele, C. (1998). *Nanofiltration as a treatment method for the removal of pesticides from ground waters*. Desalination 117(1–3), 139–147.

69. Kiso, Y., Kitao, T., and Nishimura, K. (1999a). *Adsorption properties of cyclic compounds on cellulose acetate.* J. Appl. Polym. Sci. 71, 1657–1663.

70. Bowen, W. R., and Welfoot, J. S. (2005). *Modelling the performance of nanofiltration membranes.* In A. I. Scha¨fer, A. G. Fane, and T. D., Waite (Eds.), Nanofiltration—Principles and Applications. Elsevier, Oxford.

71. Braeken, L., Ramaekers, R., Zhang, Y., Maes, G., Van der Bruggen, B., and Vandecasteele, C. (2005b). *Influence of hydrophobicity on retention in nanofiltration of aqueous solutions containing organic compounds*. J. Membr. Sci. 252(1–2), 195–203.

72. Wiesner, M. R., and Chellam, S. (1999). *The promise of membrane technologies*. Environ. Sci. Technol. 33(17), 360A–366A.

73. Lee, S., and Lee, C. H. (2000). *Effect of operating conditions on CaSO4 scale formation mechanism in nanofiltration for water softening*. Water Res. 34(15), 3854–3866.

74. Her, N., Amy, G., and Jarusutthirak, C. (2000). *Seasonal variations of nanofiltration (NF) foulants: Identification and control*. Desalination 132(1–3), 143–160.

75. Vrouwenvelder, H. S., van Paassen, J. A. M., Folmer, H. C., Hofman, J. A. M. H., Nederlof, M. M., and van der Kooij, D. (1998). *Biofouling of membranes for drinking water production.* Desalination 118(1–3), 157–166.

76. Nilson, J. A., and DiGiano, F. A. (1996). *Influence of NOM composition on nanofiltration*. J. AWWA 88(5), 53–66

77. Braghetta, A., DiGiano, F. A., and Ball, W. P. (1998). *NOM accumulation at NF membrane surface: Impact of chemistry and shear*. J. Environ. Eng. ASCE 124(11), 1087–1098.

78. Baker, J., Stephenson, T., Dard, S., and Cote, P. (1995). *Characterisation of fouling of nanofiltration membranes used to treat surface waters*. Environ. Technol. 16(10), 977–985.

79. Van der Bruggen, B., Lejon, L., and Vandecasteele, C. (2003). *Reuse, treatment and discharge of the concentrate of pressure driven membrane processes.* Environ. Sci. Technol. 37(17), 3733–3738.

80a. Kiso, Y., Kitao, T., and Nishimura, K. (1999b). *Adsorption properties of aromatic compounds on polyethylene as a membrane material*. J. Appl. Polym. Sci. 74, 1037–1043.

80b. Kiso, Y., Nishimura, Y., Kitao, T., and Nishimura, K. (2000). *Rejection properties of non-phenylic pesticides with nanofiltration membranes.* J. Membr. Sci. 171, 229–237.

81. Squire, D., Murrer, J., and Holden, P. (2000). *Disposal of reverse osmosis membrane concentrate.* Desalination 132, 47–54.

82. Ahmed, M., Shayya,W. H., Hoey, D., and Al-Handaly, J. (2001). *Brine disposal from reverse osmosis desalination plants in Oman and the United Arab Emirates.* Desalination 133, 135–147.

83. Truesdall, J., Mickley, M., and Hamilton, R. (1995). *Survey of membrane drinking water plant disposal methods.* Desalination 102, 93–105.

84. Rahimpour A, S.S. Madaeni , Y. Mansourpanah, (2007) *The effect of anionic, non-ionic dan cationic surfactants on morphology dan performance of poliethersulfone ultrafiltration membrans for milk concentration,* Journal of Membran Science vol.296 hal. 110–121.

85. Skluzacek J.M, M.Isabel Tejedor, Marc A. Danerson, 2007 *NaCl rejection by an inorganic nanofiltration membran in relation to its central pore potential,* J. Membr. Sci. vol.289 hal.32-39.

86. Suresh G., A.K. Pdaney, A. Goswami, 2007 *Permeability of water in poli(perfluorosulfonic) acid membran with different counterions*, Journal of Membran Science vol. 295 hal.21–27.

87. Kailash C. Khulbe, C.Y. Feng, Takeshi Matsuura, *Synthetic Polymeric Membranes* 2008 Springer-Verlag Berlin Heidelberg,

88. Christian, Sherril Duane, *Solubilization in Surfactant Aggregates Surfactant Science*, 1995 CRC Press New York 100-132

89. Fengel D, Wegener G. 1984. *Wood: Chemistry, Ultrastructure, Reaction*. Berlin: Walter de Gruyter.